Int J Earth Sci (Geol Rundsch) (2011) 100:695–715
DOI 10.1007/s00531-010-0527-0

REVIEW ARTICLE

Geochemical syntheses among the cratonic, off-cratonic and orogenic garnet peridotites and their tectonic implications

Benxun Su · Hongfu Zhang · Yanjie Tang ·
Benny Chisonga · Kezhang Qin · Jifeng Ying ·
Patrick Asamoah Sakyi

Received: 28 August 2009 / Accepted: 31 January 2010 / Published online: 11 March 2010

Abstract Garnet-bearing mantle peridotites, occurring as either xenoliths in volcanic rocks or lenses/massifs in high-pressure and ultrahigh-pressure terrenes within orogens, preserve a record of deep lithospheric mantle processes. The garnet peridotite xenoliths record chemical equilibrium conditions of garnet-bearing mineral assemblage at temperatures (T) ranging from * 700 to 1,400°C and pressures (P) of 1.6–8.9 GPa, corresponding to depths of * 52–270 km. A characteristic mineral paragenesis includes Cr-bearing pyropic garnet (64–86 mol% pyrope; 0–10 wt% Cr_2O_3), Cr-rich diopside (0.5–3.5 wt% Cr_2O_3), Al-poor orthopyroxene (0–5 wt% Al_2O_3), high-Cr spinel (Cr/(Cr + Al) 9 100 atomic ratio = 2–86) and olivine (88–94 mol% forsterite). In some cases, partial melting, re-equilibration involving garnet-breakdown, deformation, and mantle metasomatism by kimberlitic and/or carbonatitic melt percolations are documented. Isotope model ages of Archean and Proterozoic are ubiquitous, but Phanerozoic model ages are less common. In contrast, the orogenic peridotites were subjected to ultrahigh-pressure (UHP) metamorphism at temperature ranging from * 700 to 950 °C and pressure of [3.5–5.0 GPa, corresponding to depths of [110–150 km. The petrologic comparisons between 231 garnet peridotite xenoliths and 198 orogenic garnet peridotites revealed that (1) bulk-rock REE (rare earth element) concentrations in xenoliths are relatively high, (2) clinopyroxene and garnet in orogenic garnet peridotites show a highly fractionated REE pattern and Ce-negative anomaly, respectively, (3) Fo contents of olivines for off-cratonic xenolith are in turn lower than those of orogenic garnet and cratonic xenolith but mg-number of garnet for orogenic is less than that of off-cratonic and on-cratonic xenolith, (4) Al_2O_3, Cr_2O_3, CaO and Cr# of pyroxenes and chemical compositions of whole rocks are very different between these garnet peridotites, (5) orogenic garnet peridotites are characterized by low T and high P, off-cratonic by high T and low P, and cratonic by medium T and high P and (6) garnet peridotite xenoliths are of Archean or Proterozoic origin, whereas most of orogenic garnet peridotites are of Phanerozoic origin. Taking account of tectonic settings, a new orogenic garnet peridotite exhumation model, crust-mantle material mixing process, is proposed. The composition of lithospheric mantle is additionally constrained by comparisons and compiling of the off-cratonic, on-cratonic and orogenic garnet peridotite.

Keywords Craton and off-craton · Garnet peridotite xenolith · Orogenic garnet peridotite · Lithospheric mantle

B. Su (&) · K. Qin
Key Laboratory of Mineral Resources,
Institute of Geology and Geophysics, Chinese Academy of Sciences, P.O. Box 9825, 100029 Beijing, China
e-mail: subenxun@mail.igcas.ac.cn

B. Su · H. Zhang · Y. Tang · J. Ying
State Key Laboratory of Lithospheric Evolution,
Institute of Geology and Geophysics, Chinese Academy of Sciences, P.O. Box 9825, 100029 Beijing, China

B. Su
Graduate University of Chinese Academy of Sciences, 100049 Beijing, China

B. Chisonga
Snowden Mining Industry Consultants, Technology House, Parklands, Box 2613, 2121 Johannesburg, South Africa

P. A. Sakyi
Department of Geology, University of Ghana, P.O. Box LG 58, Legon-Accra, Ghana

Introduction

Garnet peridotite dominates the lower portion of lithospheric mantle and most of the asthenosphere and provides a record for numerous events, e.g., a source of abundant ma c and ultra-ma c magmas and mantle plumes (e.g., Sun and McDonough 1989; Salters 1996; Litasov et al. 2000; Kerrich and Polat 2006). Once some events (i.e., upwelling or melting) take place in the mantle, garnet peridotite would respond rstly in terms of partial melting or metasomatism. During the fast-ascent of asthenosphere-derived magma, the fragments of lithospheric mantle could be trapped and transported to the surface. Previous studies suggested that an important way to produce basaltic magma is the melting of lithospheric mantle (Jahn et al. 1999; Schiano et al. 2000; Sagong et al. 2001) and lithospheric mantle could be modi ed by the interaction between peridotite and melt/ uids (Grif n et al. 1992; Zhang 2005; Tang et al. 2006; Zhang et al. 2007a, b, c, 2008). In addition, peridotite fragment hosted in magma might experience compositional and structural changes (Downes 1990; Schmidberger and Francis 1999; Su et al. 2006, 2010; Carlson et al. 2007; Zhang et al. 2006, 2007a, b, 2008), although they ascend very fast. Garnet peridotite xenoliths that many researchers have investigated may be involved in all of these processes and subsequently could provide important clues to the structure, nature and evolution of lithosphere, asthenosphere and the magma genesis. Thus, the deep processes of the upper mantle could be known through investigations of these xenoliths and xenocrysts.

Studies of orogenic peridotite provide an additional window into upper mantle processes at convergent plate margins. The subduction of continental material to depths greater than 200 km is possible, and some fragments of the subducted lithosphere are exhumed to the orogenic belt and subjected to high-pressure metamorphism (Van Roermund and Drury 1998; Van Roermund et al. 2001; Ye et al. 2000). Therefore, peridotites involved preserve records of ultra-deep origin (Zhang et al. 2003, 2004a, b). Meanwhile, recent studies indicate that many orogenic peridotites were derived from a depleted and metasomatized mantle and then subjected to high-pressure metamorphism (e.g., Jahn 1998; Zhang and Liou 1998; Zhang et al. 2000a, b, 2003). However, some researchers suggested that some orogenic peridotites represent the peridotites from the mantle wedge above a subduction zone which sank and were incorporated in subducted continental crust or products of subduction-zone metamorphism of peridotite previously emplaced into the crust (e.g., Chemenda et al. 1996; Burov et al. 2001; Boutelier et al. 2004; Liou et al. 2007; Warren et al. 2008). The following issues are still controversial and need further study: (1) whether protoliths of orogenic garnet peridotites originate from lithospheric mantle or not? (2) If so, how can we nd the original records which were likely to be covered by subsequent modi cations? (3) How were these garnet peridotites at great depths incorporated into the subduction zone and then brought to the surface? and (4) How do the tectonic processes modify the garnet peridotites and are there some different compositions from garnet peridotite xenoliths?

In any case, garnet peridotites can be collected both in cratons and in convergent boundaries, particularly orogenic belts, and provide an important window to probe mantle processes. Diamond is found in garnet peridotite xenoliths and especially in orogenic garnet peridotites as reported recent years (e.g., Chopin 1984; Smith 1984; Van Roermund et al. 2001; Zhang et al. 2003, 2004a, b; Yang 2003; Song et al. 2005, 2007). Thus, it has become a hot issue to investigate the origin and evolution of garnet peridotites. In this paper, we compile the published and unpublished major and trace element data of global garnet peridotites occurring as xenoliths in the off-craton and on-craton and fragments in orogenic belts and try to understand their different evolution by compositional and tectonic comparisons.

Global distribution of garnet peridotite

Garnet peridotite occurs mainly in two different ways, as xenoliths or as orogenic garnet peridotite lens/massifs: (1) garnet peridotite xenolith: the magma originating from the base of lithosphere (i.e., basalt), particularly from deeper asthenosphere (i.e., kimberlite), usually brings up some garnet peridotite fragments while ascending to the surface. Basically, the tectonic settings where garnet peridotite xenoliths occur can be distinguished as craton and off-craton. (2) orogenic garnet peridotite lens/massif: orogenic belts, due to collision and/or subduction between cratons and/or blocks, can carry masses of garnet peridotite from lithospheric mantle. However, some orogenic garnet peridotite lenses/massifs are not derived from protoliths of garnet peridotite but from other facies rocks such as spinel peridotite and cumulates, by ultra-high-pressure metamorphism (e.g., Zhang et al. 2003, 2004a, b, 2007c; Liou et al. 2004).

Garnet peridotite xenoliths in volcanic rocks

Overall, global garnet peridotite xenoliths occur within or near the margin of Archean terranes and are named herein off-cratonic and on-cratonic xenoliths, respectively (Fig. 1; Table 1). Along the eastern Euro-Asian plate, especially in eastern China, which is known as the large-scale thinning of lithosphere beneath the eastern North China Craton from [200 km to present 60–80 km (Grif n et al. 1992; Menzies et al. 1993; Xu et al. 1996, 2003; Fan et al. 2000; Zheng et al. 2004; Zhang 2005; Ying et al. 2006; Chen et al. 2006;

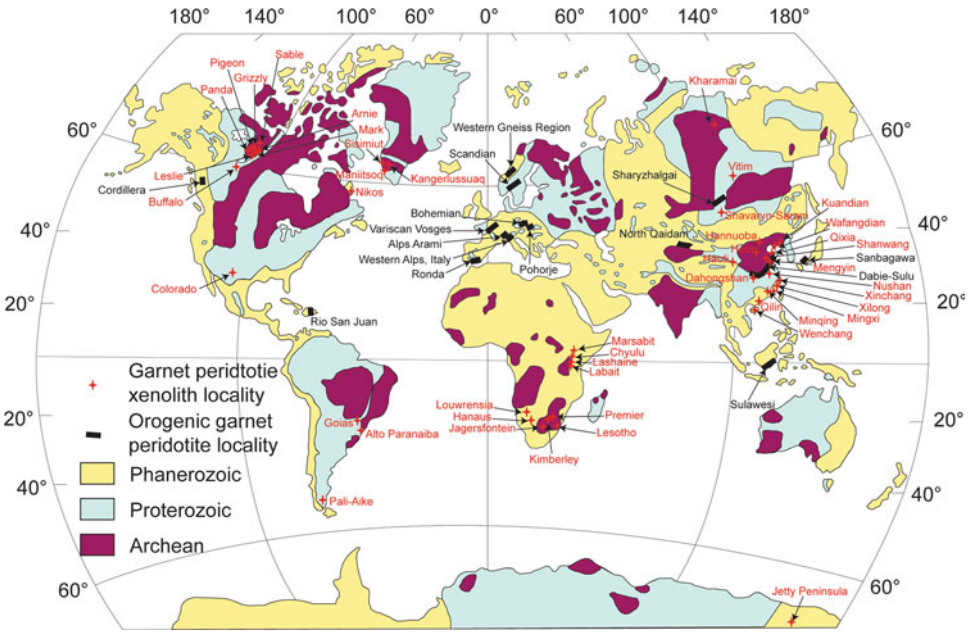

Fig. 1 Distributions of global garnet peridotite xenoliths and orogenic garnet peridotites (modi ed after Kerrich and Polat 2006)

Zhang et al. 2006, 2007a, b, 2008), many garnet peridotite xenoliths occurred from north Siberia (Russia) to the south Cathaysia block (China) (Fig. 1), but the amounts of garnet peridotites are less abundant than those in Tanzania (Tanzania), Kaapvaal (South Africa) and Slave (Canada) craton where a thick [(150 km) lithosphere is still preserved at present (Henjes Kunst and Altherr 1992; Simon et al. 2003; Kopylova and Caro 2004; Menzies et al. 2004; Liati et al. 2004; Boyd et al. 2004; Viljoen et al. 2005). The occurrence of all almost garnet peridotite xenoliths is related to subduction zones (e.g., eastern China) (e.g., Zheng et al. 2006) or mantle plumes (e.g., Tanzania craton) (e.g., Henjes Kunst and Altherr 1992; Chesley et al. 1999).

Garnet peridotites in the lower part of lithospheric mantle need great drive-force to breakdown and fast erupting host magma to carry them. Thus, kimberlite and alkali basalt usually host garnet peridotite xenoliths (Table 1). The exception, however, is kamafugite in Haoti, China, and in Gioas and Alto Paranaiba, Brazil, and an karamite in Lashaine, Tanzania (Yu 2004; Junqueira Brod et al. 2005; Carlson et al. 2007; Su et al. 2009, 2010). Kamafugites always coexist with carbonatite but their origin is controversial (Yu 2004; Junqueira Brod et al. 2005; Carlson et al. 2007). Most kimberlites (except Buffalo in Canada) and all kamafugites outcrop in craton and off-craton, respectively, and other host rocks occur in both tectonic settings (Table 1). Perhaps, garnet peridotite xenoliths could give some implications for the origin depth and genesis of these host rocks.

Most kimberlites hosting garnet peridotite erupted during Paleozoic (Wafangdian, Mengyin, Dahongshan in China) and Mesozoic (Kharamai in Russia, Buffalo Head terrane and Nikos in Canada, Jetty Peninsula in Antarctic, Louwrensia and Hanaus in Namibia, Premier and Kimberley in South Africa and Lesotho) (Table 1). Greenland and Slave craton (Canada) kimberlites give Proterozoic and Cenozoic ages, respectively. Alkali basalts, kamafugites (except Brazil), and ankaramites erupted during Cenozoic age (Table 1). Dating of garnet peridotite xenoliths by different isotopic systems has yielded Archean to Proterozoic ages.

Orogenic garnet peridotite lenses/massifs

Since diamond was discovered in garnet peridotite massifs in western Alps and Western Gneiss Region of Norway (Chopin 1984; Smith 1984), orogenic garnet peridotites especially in ultrahigh-pressure metamorphic belt have been a hot topic. In the past decades of years, geologists have identi ed several new garnet peridotite localities involving the well-known Alps and Dabie-Sulu belts, as well as the Sharyzhalgai in Russia (Ota et al. 2004), Scandian in Sweden (Brueckner et al. 2004) and North Qaidam in China (Song et al. 2004, 2005, 2007).

The orogenic garnet peridotites are merely distributed in the Euro-Asian plate (Fig. 1) and usually occurred as layers, lenses or massifs coexisting with eclogite, granulite and gneiss (Table 1). A remarkable characteristic is that the age of orogenic garnet peridotite is mostly consistent with the peak metamorphism age of orogenic belt (except Scandian in Sweden and Sulawesi in Indonesia) (Table 1).

The distribution of worldwide garnet peridotites is compiled in Fig. 1 and Table 1. Their occurrences and tectonic settings are brie y illustrated in Fig. 2 and summarized as follows: (1) garnet peridotite xenoliths outcropping within craton are mostly entrained in ultrama c

Table 1 Summary of garnet peridotite distributions in the world

Locality	Tectonic	Host rock	Age of host rock	Age of peridotite	Data source
Garnet peridotite xenolith					
Asia					
Vitim, Russia	Off-craton	Alkali basalt	Cenozoic	Proterozoic	Ionov et al. (1993, 2005), Ionov (2004), Glaser et al. (1999), Litasov et al. (2000)
Kharamai, Russia	Craton	Kimberlite	Mesozoic	Proterozoic	Grif n et al. (2005)
Shavanryn-Saram, Mongolia	Off-craton	Alkali basalt	Cenozoic	Proterozoic	Deng and Macdougall (1992), Kopylova et al. (1995)
Wafangdian, China	Craton	Kimberlite	Paleozoic	Archean	E and Zhao (1987), Zhang et al. (2000a), Gao et al. (2002), Wu et al. (2006)
Mengyin, China	Craton	Kimberlite	Paleozoic	Proterozoic	Zhang et al. (2000a, b), Gao et al. (2002), Wu et al. (2006)
Dahongshan, China	Craton	Kimberlite	Paleozoic	Proterozoic	Zhang et al. (2001)
Kuandian, China	Craton	Alkali basalt	Cenozoic	Archean	E and Zhao (1987), Wu et al. (2006)
Hannuoba, China	Craton	Alkali basalt	Cenozoic	Proterozoic	Liu et al. (1985), Fan and Liu (1990), Jin and Pan (1998), Li et al. (1999), Zhi and Qin (2004)
Qixia, China	Craton	Alkali basalt	Cenozoic	Proterozoic	Fan and Liu (1990), Zheng et al. (2006), Zhi and Qin (2004)
Shanwang, China	Craton	Alkali basalt	Cenozoic	Proterozoic	E and Zhao (1987), Zheng et al. (2006), Zhi and Qin (2004)
Hebi, China	Craton	Alkali basalt	Cenozoic	Proterozoic	Fan and Liu (1990)
Nushan, China	Craton	Alkali basalt	Cenozoic	Proterozoic	Xu et al. (1998, 2003), Huang et al. (1998), Zhi et al. (2001)
Haoti, China	Off-craton	Kamafugite	Cenozoic	?	Yu et al. (2001), Su et al. (2007)
Xinchang, China	Off-craton	Alkali basalt	Cenozoic	Proterozoic	Liu et al. (1985), Lin et al. (1995), Zhi (2000)
Xilong, China	Off-craton	Alkali basalt	Cenozoic	Proterozoic	Cao and Zhao (1990), Zhi (2000)
Mingxi, China	Off-craton	Alkali basalt	Cenozoic	Proterozoic	Zhang and Cong (1985), Fan and Hooper (1989), Xu (2000), Zhi (2000)
Minqing, China	Off-craton	Alkali basalt	Cenozoic	Proterozoic	Liu et al. (1985), Zhang and Cong (1985), Fan and Hooper (1989), Zhi (2000)
Qilin, China	Off-craton	Alkali basalt	Cenozoic	Proterozoic	E and Zhao (1987), Xu et al. (1996), Zhi (2000)
Wenchang, China	Off-craton	Alkali basalt	Cenozoic	Proterozoic	Fan and Hooper (1989), Zhi (2000)
Africa					
Marsabit and Chyulu, Kenya	Off-craton	Basalt	Cenozoic	Proterozoic	Henjes Kunst and Altherr (1992)
Lashaine and Labait, Tanzania	Craton	Ankaramite and carbonitite	Cenozoic	Proterozoic	Reid et al. (1975), Rhodes and Dawson (1975), Ridley and Dawson (1975), Bishop et al. (1978), Henjes Kunst and Altherr (1992), Su (unpublished data)
Louwrensia and Hanaus, Namibia	Off-craton	Kimberlite	Mesozoic	Proterozoic	Liati et al. (2004), Boyd et al. (2004)
Premier, Kimberley, South Africa	Craton	Kimberlite	Mesozoic	Archean	Bishop et al. (1978), Simon et al. (2003), Viljoen et al. (2005)
Lesotho	Craton	Kimberlite	Mesozoic	Archean	Bishop et al. (1978), Saltzer et al. (2001), Simon et al. (2003)
America					
Sable, Pigeon, Grizzly, Arnie, Mark, Panda and Leslie, Canada	Craton	Kimberlite	Cenozoic	Archean	Menzies et al. (2004)
Buffalo Head Terrane, Canada	Off-craton	Kimberlite	Mesozoic	Proterozoic	Aulbach et al. (2004), Hood and McCandless (2004)

Table 1 continued

Locality	Tectonic	Host rock	Age of host rock	Age of peridotite	Data source
Nikos, Canada	Craton	Kimberlite	Mesozoic	Archean	Schmidberger and Francis (1999)
Colorado, America	Off-craton	Ultrama c breccias	Cenozoic	Proterozoic	Hunter and Smith (1981), Ehrenberg (1982), Smith and Ehrenberg (1984), Smith et al. (1991), Roden and Shimizu (2000)
Gioas and Alto Paranaiba, Brazil	Off-craton	Kamafugite	Mesozoic	Proterozoic	Carlson et al. (2007)
Pali-Aike	Off-craton	Alkali basalt	Cenozoic	Proterozoic	Stern et al. (1999)
Atlantic craton					
Sisimiut, Maniitsoq and Kangerlussuaq, Greenland	Craton	Kimberlite	Proterozoic	Archean	Bizzarro and Stevenson (2003)
Antarctic craton					
Jetty Peninsula, Antarctica	Craton	Alkali basalt	Mesozoic	Proterozoic	Foley et al. (2006)

Locality	Occurrence	Coexistent rock	Age of peridotite		Data source
Orogenic garnet peridotite					
North Qaidam, China	Layer	Eclogite and gneiss	Paleozoic	Paleozoic	Song et al. (2004, 2005, 2007)
Dabie-Sulu, China	Massif	Eclogite and gneiss	Mesozoic	Mesozoic	Zhang et al. (1994, 2000b, 2003, 2004a, b, 2005, 2007a), Zhang and Liou (1998), Liu et al. (1995), Hacker et al. (1997), Liou and Zhang (1998), Yang and Jahn (2000), You et al. (2000), Yang (2003), Yoshida et al. (2004), Zheng et al. (2005, 2006), Xu et al. (2006), Yang et al. (2007), Zhao et al. (2007)
Sanbagawa, Japan	Massif	Eclogite and gneiss	Mesozoic	Mesozoic	Isozaki et al. (1994), Kawato et al. (1991), Yamamoto et al. (2004), Enami et al. (2004)
Sulawesi, Indonesia	Massif	Granulite and eclogite	Cenozoic	Mesozoic	Kadarusman and Parkinson (2000), Helmers et al. (1990)
Sharyzhalgai, Russia	Lens	Granulite	Proterozoic	Proterozoic	Ota et al. (2004)
Cordillera, Canada	Massif	Eclogite	Mesozoic	Mesozoic	MacKenzie et al. (2005)
Rio San Juan, Dominican	Lens	Gneiss and eclogite	Cenozoic	Cenozoic	Draper and Nagle (1991), Abbott et al. (2005a, b, 2006), Abbott and Draper (2007)
Alpe Arami, Switzerland	Massif	Greenchist and eclogite	Cenozoic	Cenozoic	Green et al. (1997), Nimis and Trommsdorff (2001); Paquin and Altherr (2001)
Ronda, Spain	Massif	Eclogite and granulite	Cenozoic	Cenozoic	Obata (1980), Lenoir et al. (2001), Morishita et al. (2001), Villasante-Marcos et al. (2003)
Pohorje, Slovenia	Massif	Eclogite	Mesozoic	Mesozoic	Janak et al. (2006)
Western Gneiss Region, Norway	Massif	Gneiss and eclogite	Proterozoic	Proterozoic	Van Roermund et al. (2001), Beyer et al. (2006), Spengler et al. (2006)
Western Alps, Italy	Lens	Gneisses and migmatites	Cenozoic	Cenozoic	Obata and Morten (1988), Godard et al. (1996), Rampone and Morten (2001), Godard and Martin (2000), Nimis and Morten (2000)
Scandian, Sweden	Lens	Gneiss and schist	Paleozoic	Archean	Brueckner et al. (2004)
Bohemian, Austria and Czech	Massif	Granulite and gneiss	Paleozoic	Paleozoic	Becker (1996), Medaris et al. (2005)
Variscan Vosges, France	Lens	Granulite and eclogite	Paleozoic	Paleozoic	Altherr and Kalt (1996)

Orogenic garnet peridotites from Sanbagawa, Japan and Rio San Juan, Dominacan have no data published and special compositions i.e. quite low Mg# in main minerals, respectively, therefore they don't present in the diagrams below

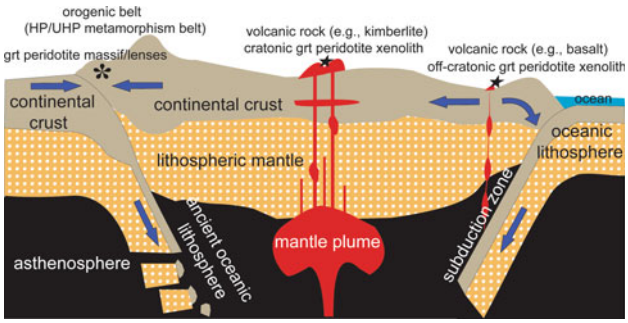

Fig. 2 Garnet peridotite occurrences and their possibly relatec tectonic setting

volcanic rocks (mainly kimberlites), which erupted gener-ally in Paleozoic or earlier within these areas preservinç thick lithosphere and are basically related to low-degree partial melting of lower mantle and/or mantle plume; (2) off-cratonic garnet peridotite xenoliths are hosted within ma c and alkaline volcanic rocks (mainly alkaline basalts), which are distributed within the margin of cratons and should be closely related to active lithospheric mantle anc extensive settings; and (3) orogenic garnet peridotite len ses/massif are certainly located within orogenic belts anc represent the response to the subduction and late-sta continental collision.

Compositional comparisons of garnet peridotites

Major and trace element compositions of 231 garnet peri dotite xenoliths (134 from craton and 97 from off-craton) and 198 orogenic garnet peridotites from 127 literatures have been compiled (Table 1; e.g., Ionov et al. 1993, 2005; Ionov 2004; Yang and Jahn 2000; Zhang et al. 2000a, b; Nimis and Trommsdorff 2001; Gao et al. 2002; Brueckner et al. 2004; Menzies et al. 2004; Song et al. 2004, 2005, 2007; Grif n et al. 2005; Wu et al. 2006; Carlson et al. 2007).

Major element

Olivine

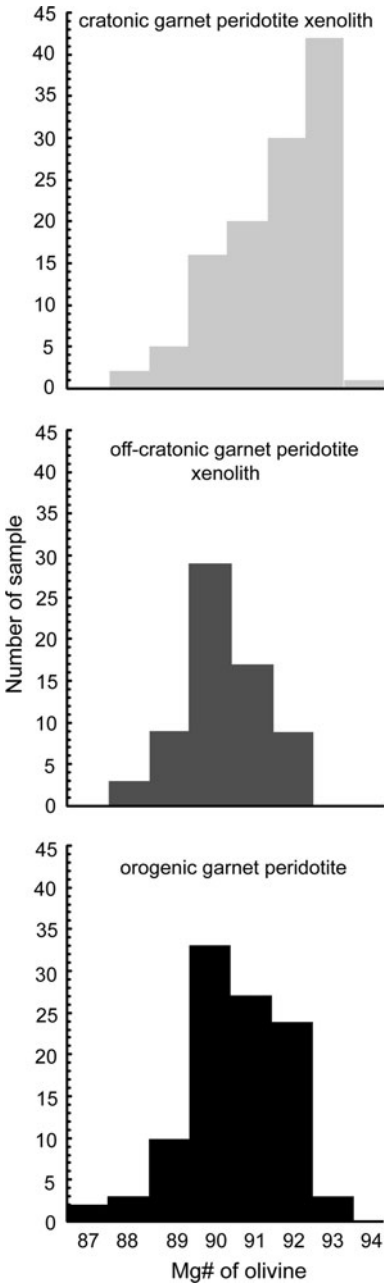

Fig. 3 Mg# of olivine versus amount of garnet peridotites

From the statistic diagram, Fo contents of olivines from different occurrences are identi ed with variable peaks and ranges (Fig. 3). Olivines from cratonic garnet peridotite xenoliths have a large Mg# range (88–94) with a peak of 92–93. The majority of olivines from off-cratonic garnet peridotite xenoliths have a 90 Mg# peak in the relatively narrow range (88–92). Fo contents of these olivines in basalt are lower than those in kimberlite. Fo contents of olivines in orogenic garnet peridotites show a large range of 87–93 with peaks of 90–92. In addition, CaO contents of olivines are in the range of 0–0.15 wt% (0–0.06 wt% in kimberlite and 0.06–0.15 wt% in basalt), 0.05–0.15 wt% and 0–0.03 wt% in cratonic, off-cratonic and orogenic garnet peridotites, respectively.

Orthopyroxene

Orthopyroxenes in off-cratonic garnet peridotite have lower Mg#, Cr# and higher CaO, Cr_2O_3 and Al_2O_3 contents than those in cratonic garnet peridotite entrained in kimberlite but similar to those in basalt and ankaramite (Fig. 4). Although cratonic and off-cratonic orthopyroxenes cannot be classi ed, the Al_2O_3 content displays an apparent boundary

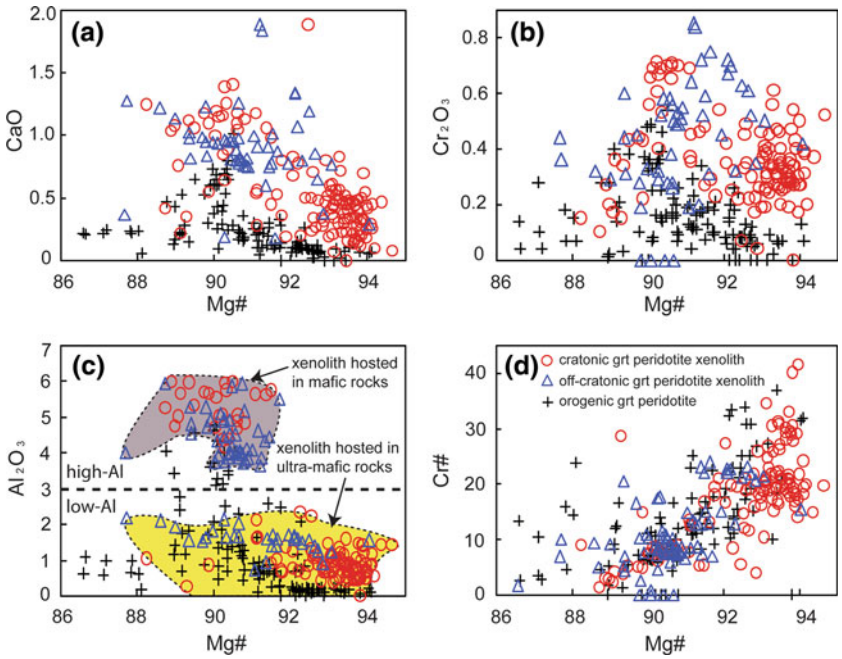

Fig. 4 Major elements of orthopyroxenes in garnet peridotites. The same symbols are used in following diagrams

between orthopyroxenes from ultra-mafic (< 3 wt%) and mafic (> 3 wt%) host rocks (Fig. 4c), which are marked as low-Al and high-Al groups. In orogenic garnet peridotites, orthopyroxenes are characterized by large variation Mg# and low CaO, Cr_2O_3 and Al_2O_3 in the same Mg# levels compared with those in xenoliths. CaO, Cr_2O_3, Al_2O_3 and TiO_2 contents increase with the increasing Mg# but decrease with the increasing Mg#s from 90 to 94 (Fig. 4a–c). However, Cr contents show significantly positive correlations with Mg-number for the three garnet peridotite types (Fig. 4d).

Clinopyroxene

The compositions of clinopyroxene in the garnet peridotites display distinct variations. Clinopyroxenes in off-cratonic garnet peridotite xenoliths, except some localities (e.g., Kenya, Namibia and Buffalo, Canada), have high Al_2O_3 (> 4 wt%) and low Mg# (< 92), similar to those in cratonic garnet peridotite xenoliths in basalt and ankaramite (Fig. 5a, b). Corresponding to the classification of orthopyroxenes, Al_2O_3 content (4 wt%) is also a key indicator to distinguish these from ultra-mafic (low-Al) and mafic (high-Al) rocks. Clinopyroxenes in orogenic garnet peridotites and cratonic garnet peridotite xenoliths display similar variations of major oxides, especially for CaO and Al_2O_3, but the former have the highest Wo (generally > 45) (Fig. 5c). The correlation between Cr# and Mg# of clinopyroxenes is not very clear, distinctive from the pattern in clinopyroxene. Generally, there is a positive correlation between Cr# and Mg# of clinopyroxenes from cratonic and off-cratonic xenoliths, whereas a scatter pattern is shown for orogenic garnet peridotite, as shown in Fig. 5d.

Garnet

Garnets in garnet peridotite xenoliths have similar Mg# and Grs (grossular) variations, but garnets in cratonic garnet peridotite xenoliths in kimberlite have relatively high Cr_2O_3, TiO_2 and Cr/Ca compared with those in basalt and ankaramite and off-cratonic ones (Fig. 6). Apparently, garnets in orogenic garnet peridotites are characterized by lower Mg# (< 84) but similar Cr_2O_3, Grs and Cr/Ca values than garnets in those xenoliths in kimberlite.

Whole rock

Whole rock Al_2O_3 ? CaO against MgO of off-cratonic garnet peridotite xenoliths appear to show steeper trend than those of cratonic garnet peridotite xenoliths (Fig. 7a). The cratonic garnet peridotite xenoliths have higher MgO, Mg# and lower Na_2O, Al_2O_3 ? CaO contents, whereas orogenic garnet peridotites have relatively high Al_2O_3 ? CaO and Na_2O but low MgO and Mg# (Fig. 7b).

REE element

Clinopyroxenes in off-cratonic garnet peridotite show convex-upward chondrite-normalized REE patterns with depleted HREE and low La_N/Yb_N ratios (< 8). Meanwhile, clinopyroxenes in cratonic garnet peridotite and in orogenic garnet peridotite with Yb-negative anomalies have higher LREE abundances and La_N/Yb_N ratios (> 11) than those of off-cratonic clinopyroxenes.

Garnets in both cratonic and off-cratonic garnet peridotites have similar REE pattern and higher REE

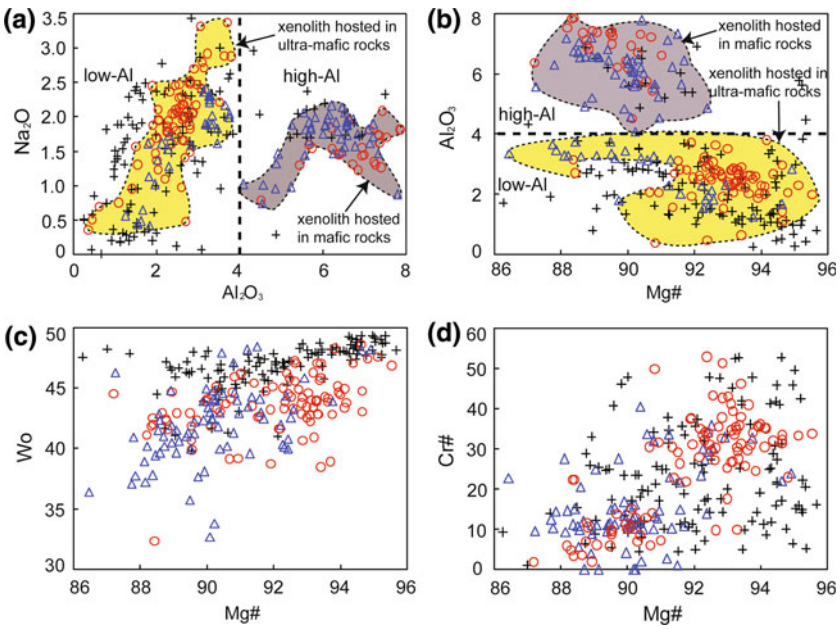

Fig. 5 Major elements of clinopyroxenes in garnet peridotites

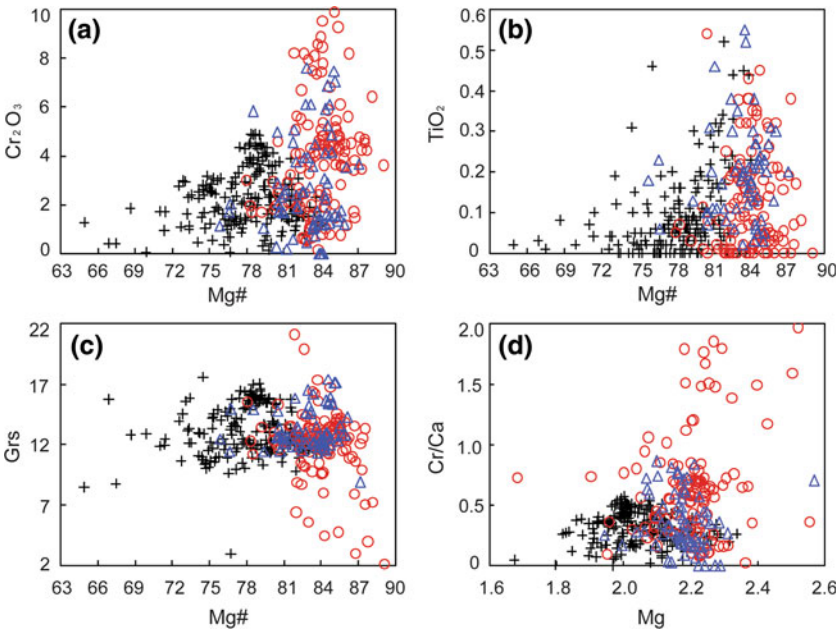

Fig. 6 Major elements of garnets in garnet peridotites. Grs grossular

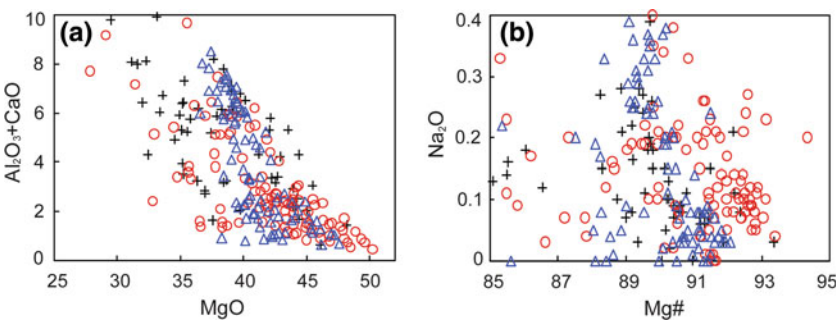

Fig. 7 Major elements of garnet peridotites

(especially HREE) abundances in comparison with those in orogenic garnet peridotites. REE abundances of garnets in cratonic and off-cratonic garnet peridotites show large variations and LREE depletions (Fig. 8c). All garnets in orogenic garnet peridotites have remarkable Ce-negative anomalies that are absent in garnet peridotite xenoliths.

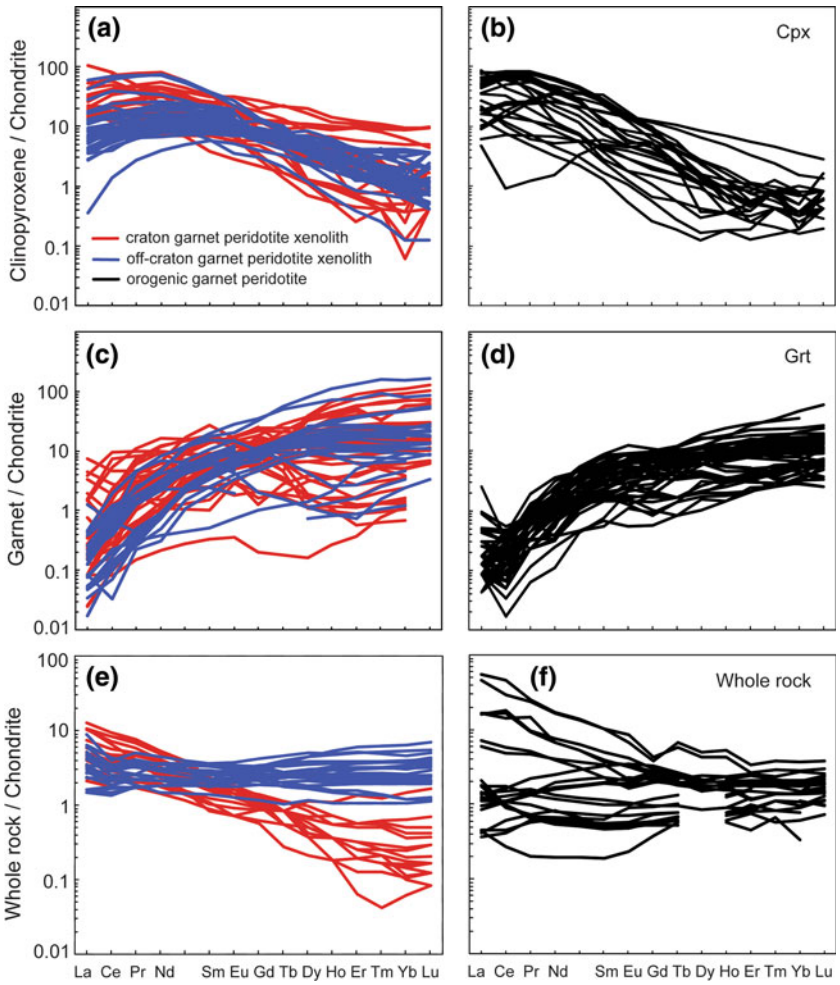

Fig. 8 Chondrite-normalized REE of Cpx, Grt and whole rock of garnet peridotite xenoliths (left) and orogenic garnet peridotite (right). Chondrite-normalized values are from (Sun and McDonough 1989)

Overall, HREE abundances of off-cratonic garnet peridotite xenoliths are higher than those of cratonic garnet peridotite xenoliths and orogenic garnet peridotites. REE patterns of off-cratonic garnet peridotite xenoliths are quite flat and those of cratonic garnet peridotite xenoliths show highly fractionated. REE distributions in orogenic garnet peridotites are slightly scattered.

P–T

In this paper, we recalculate temperature and pressure of garnet peridotite using single orthopyroxene-garnet geothermobarometry (Brey and Kohler 1990) and the results are shown in Fig. 9.

Off-cratonic garnet peridotite xenoliths (except samples from Kenya, Namibia and Buffalo, Canada) show high temperatures (950–1,250 °C) and low pressures (1.7–3.2 GPa), and the highest pressures are from the samples in kamafugite from Haoti, China. Just like the major element distribution of minerals, cratonic garnet peridotite xenoliths in basalt and ankaramite plot in the P–T field of off-cratonic ones. Garnet peridotite xenoliths hosted in mafic rocks (high-Al group) plot above the oceanic geothermal line whereas those hosted in ultra-mafic rocks (low-Al group) plot along the continental geothermal line. Most of the orogenic garnet peridotites are characterized by low temperatures (600–900 °C) and relatively high pressure (some up to 10 GPa), although some plot in the P–T field of garnet peridotite xenoliths.

Discussion

Further constraints on the composition of lithospheric mantle

The average compositions for garnet peridotite xenoliths from both craton and off-craton and spinel peridotite xenolith (Maaloe and Aoki 1977) shown in Table 2 might be representative of the lower and upper compositions of the lithospheric mantle, respectively. The garnet peridotite xenolith has relatively higher Al_2O_3 and CaO contents than those estimates by the average of modal and mineral compositions (Maaloe and Aoki 1977) but lower than

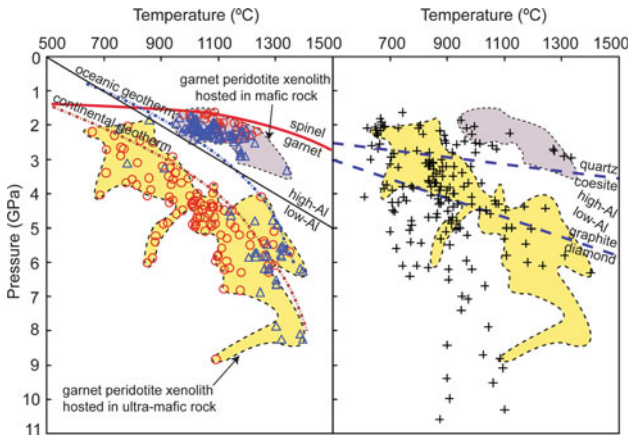

Fig. 9 Recalculated temperatures and pressures of garnet peridotites. The garnet-spinel line is from Klemme (2004); The quartz-coesite line is from Liou et al. (2007); The graphite-diamond line and oceanic and continental geothermal lines are from Menzies and Chazot (1995)

spinel peridotite xenolith (Table 2). However, Mg#s of the average (this study) and estimated garnet peridotites (90.4 and 90.6) are slightly higher than spinel peridotite xenolith (89.7) and primitive mantle (88.8) (Maaloe and Aoki 1977; Sun and McDonough 1989). Compared to the primitive mantle composition, the average compositions of all peridotite xenoliths are enriched in MgO and depleted in TiO_2, Al_2O_3, Cr_2O_3, CaO and Na_2O. These features are consistent with the hypothesis that peridotite xenoliths are the residues after partial melting (Menzies and Hawkesworth 1987; McDonough and Frey 1989) and higher degrees of melting occurred in the lower garnet peridotite than in the upper spinel peridotite.

The REE patterns of garnet and spinel peridotite xenoliths display relatively coherent LREE-enrichment trends and at HREE abundances. The spinel peridotite has similar HREE abundance and higher LREE abundance than garnet peridotite (Fig. 10). The lower HREE abundance in garnet is consistent with the lower Al_2O_3 and CaO contents, reflecting higher degree of melt extraction. Higher La/Yb ratio in spinel peridotite xenolith indicates that they have either been more strongly enriched in LREE during their formation or modified/metasomatized by the melt/fluid with a higher La/Yb ratio (McDonough 1990). Lower REE abundance and La/Yb ratio in garnet peridotite xenolith than in spinel peridotite xenolith are possibly caused by different olivine and clinopyroxene modes because clinopyroxene and garnet have been postulated to be main reservoirs of REE (Stosch 1982; McDonough et al. 1992).

Compared to off-cratonic and orogenic garnet peridotites, cratonic garnet peridotite has the lowest Al_2O_3, CaO, Na_2O, FeO, Cr_2O_3, NiO and MnO contents, and the highest MgO and Mg# (91.2) and gives moderate pressure (3.2 GPa) and temperature (992 °C) (Table 2). Mg# of olivine in cratonic garnet peridotite is relatively high (91.7). CaO contents of orthopyroxenes and Al_2O_3 contents decoupled with Cr_2O_3 contents of garnets increase and decrease, respectively, from off-cratonic through cratonic to orogenic garnet peridotites, corresponding to decreasing temperature from 1,112 through 992 to 886 °C and increasing pressure from 2.8 through 3.2 to 4.08 GPa (Table 2). These characteristics indicate that cratonic garnet peridotite should have undergone relatively higher partial melting. Off-cratonic garnet peridotite is very similar to spinel peridotite xenolith in SiO_2, Al_2O_3 and CaO contents and Mg# (Table 2) and integrates the distribution near the garnet-spinel transition line in Fig. 9, suggesting that off-cratonic garnet peridotite xenolith is likely to undergo the similar processes to spinel peridotite xenolith. The MgO content (38.2 wt%) of orogenic garnet peridotite is lower than that in garnet peridotite xenolith (42.1 and 42.6 wt%) and spinel peridotite xenolith (41.4 wt%), whereas Al_2O_3 and CaO contents are higher. SiO_2 and FeO contents, Mg# and even REE abundance in orogenic garnet peridotite are very similar to those in the primitive mantle (Table 2). Moreover, orogenic garnet peridotite has relatively higher La/Yb ratio, and the clinopyroxene and garnet have the highest and the lowest La/Yb ratios, respectively. All these features further imply that high-degree metasomatism that occurred in orogenic garnet peridotite has partially obscured partial melting and other original information about the deep-seated lithospheric mantle.

Contributions to garnet peridotite: tectonic setting, host rock and temporal evolution

The differences between the cratonic, off-cratonic garnet peridotites and orogenic garnet peridotites are summarized as follows: (1) Fo contents of olivines for off-cratonic xenolith are in turn lower than those of orogenic garnet and cratonic xenolith but mg-number of garnet for orogenic is less than that of off-cratonic and on-cratonic xenolith. (2) Al_2O_3 contents of pyroxenes entrained in mafic rocks (high-Al) are remarkably higher than those in ultra-mafic rocks (low-Al), while pyroxenes and whole rocks of most orogenic garnet peridotites, although showing large major-element variations, have similar major-element contents to those entrained in kimberlite and to those in basalt and kamafugite, respectively. (3) Clinopyroxenes in orogenic garnet peridotites show similar REE patterns to those in cratonic garnet peridotites, whereas garnets in orogenic garnet peridotites have particular Ce-negative anomaly and identical and narrow-ranging REE patterns compared with those in xenoliths. However, whole rock REE patterns of orogenic garnet peridotites basically are close to those of off-craton garnet peridotite xenoliths and differ from the

Table 2 Average composition of garnet peridotite xenolith and orogenic garnet peridotite comparing with continental garnet peridotite xenolith, spinel peridotite xenolith and primitive mantle (major element, in wt%; REE, in ppm)

	Cratonic grt peridotite xenolith					Off-cratonic grt peridotite xenolith				
	WR	Ol	Cpx	Opx	Grt	WR	Ol	Cpx	Opx	Grt
SiO_2	44.1	41.1	53.9	57.0	41.9	44.1	40.8	53.2	55.6	42.0
TiO_2	0.15	0.01	0.22	0.06	0.17	0.16	0.02	0.46	0.17	0.28
Al_2O_3	1.38	0.03	3.63	1.81	20.7	2.77	0.04	4.67	3.40	21.7
Cr_2O_3	0.24	0.02	1.49	0.36	3.98	0.42	0.04	1.09	0.49	2.54
FeO_{total}	7.52	8.13	2.60	5.05	7.23	8.52	9.38	3.27	6.07	7.52
MnO	0.13	0.10	0.09	0.11	0.37	0.48	0.11	0.07	0.10	0.29
MgO	43.7	50.2	16.6	34.9	20.8	40.7	49.5	16.8	33.1	20.5
CaO	1.20	0.04	19.4	0.55	4.87	2.18	0.07	18.5	0.97	5.27
Na_2O	0.16	0.01	1.82	0.12	0.05	0.19	0.04	1.66	0.16	0.10
K2O	0.12	0.00	0.01	0.00	0.01	0.02	0.02	0.01	0.00	0.01
NiO	0.12	0.37	0.04	0.08	0.01	0.25	0.27	0.02	0.07	0.02
Total	98.9	100.1	99.8	100.0	100.1	99.7	100.3	99.7	100.2	100.3
P/T				3.2	992				2.8	1,112
Mg#	91.2	91.7	91.9	92.5	83.7	89.5	90.4	90.1	90.7	83.0
La										
Ce										
Pr										
Nd										
Sm										
Eu										
Gd										
Tb										
Dy										
Ho										
Er										
Tm										
Yb										
Lu										
ΣREE										
La/Yb										

	Grt peridotite xenolith					Orogenic grt peridotite				
	WR	Ol	Cpx	Opx	Grt	WR	Ol	Cpx	Opx	Grt
SiO_2	44.1	41.0	53.6	56.5	42.0	44.3	40.8	54.3	57.1	41.7
TiO_2	0.16	0.02	0.33	0.10	0.22	0.08	0.02	0.16	0.05	0.10
Al_2O_3	2.08	0.03	4.11	2.41	21.1	3.97	0.01	2.59	1.30	22.3
Cr_2O_3	0.34	0.03	1.31	0.41	3.37	0.38	0.03	0.92	0.17	1.54
FeO_{total}	8.01	8.60	2.91	5.43	7.35	8.45	9.57	2.30	6.41	9.97
MnO	0.27	0.10	0.08	0.11	0.34	0.14	0.12	0.06	0.13	0.45
MgO	42.1	50.0	16.7	34.2	20.7	38.2	49.2	16.2	34.6	19.2

Table 2 continued

	Grt peridotite xenolith					Orogenic grt peridotite				
	WR	Ol	Cpx	Opx	Grt	WR	Ol	Cpx	Opx	Grt
CaO	1.73	0.05	19.0	0.71	5.04	3.14	0.01	21.7	0.26	4.88
Na_2O	0.18	0.01	1.75	0.13	0.07	0.21	0.01	1.47	0.02	0.02
K2O	0.06	0.00	0.01	0.00	0.01	0.13	0.00	0.00	0.00	0.00
NiO	0.18	0.34	0.03	0.08	0.01	0.18	0.33	0.02	0.05	0.01
Total	99.2	100.1	99.7	100.1	100.2	99.2	100.1	99.7	100.1	100.2
P/T				2.98	1,041				4.08	886
Mg#	90.4	91.2	91.1	91.8	83.4	88.9	90.2	92.6	90.6	77.4
La	1.164		3.878		0.148	1.651		8.480		0.064
Ce	2.172		12.368		0.659	3.574		23.287		0.116
Pr	0.314		1.505		0.141	0.420		3.884		0.057
Nd	1.285		9.784		1.577	1.571		12.300		0.583
Sm	0.310		2.202		1.022	0.351		1.915		0.534
Eu	0.108		0.688		0.468	0.115		0.433		0.265
Gd	0.368		1.725		2.059	0.350		1.043		0.990
Tb	0.066		0.265		0.536	0.069		0.075		0.208
Dy	0.434		1.202		3.916	0.556		0.450		2.044
Ho	0.097		0.202		1.300	0.092		0.042		0.513
Er	0.269		0.453		3.383	0.241		0.140		1.844
Tm	0.043		0.060		0.463	0.040		0.017		0.292
Yb	0.281		0.333		4.006	0.269		0.108		2.334
Lu	0.045		0.054		0.816	0.044		0.019		0.380
ΣREE	6.933		34.718		20.860	9.345		52.192		10.226
La/Yb	4.135		11.636		0.037	6.136		78.371		0.028

	Continental grt peridotite xenolith	Sp peridotite xenolith	Primitive mantle
SiO_2	45.0	44.0	44.8
TiO_2	0.06	0.09	0.21
Al_2O_3	1.40	2.27	4.45
Cr_2O_3	0.32	0.39	0.43
FeO_{total}	7.89	8.43	8.40
MnO	0.11	0.14	0.14
MgO	42.6	41.4	37.2
CaO	0.82	2.15	3.60
Na_2O	0.11	0.24	0.34
K2O	0.00	0.05	0.03
NiO	0.26	0.27	0.24
Total	98.6	99.4	99.8
P/T			
Mg#	90.6	89.7	88.8
La		2.600	0.687

Table 2 continued

	Continental grt peridotite xenolith	Sp peridotite xenolith	Primitive mantle
Ce		6.290	1.775
Pr		0.560	0.276
Nd		2.670	1.354
Sm		0.470	0.444
Eu		0.160	0.168
Gd		0.600	0.596
Tb		0.070	0.108
Dy		0.510	0.737
Ho		0.120	0.164
Er		0.300	0.480
Tm		0.038	0.074
Yb		0.260	0.493
Lu		0.043	0.074
ΣREE		14.691	7.430
La/Yb		10.000	1.394

Amount of samples for average, cratonic garnet peridotite xenolith: WR (whole rock), 105; Ol, 116; Cpx, 95; Opx, 124; Grt, 133; off-cratonic garnet peridotite xenolith: WR, 85; Ol, 71; Cpx, 82; Opx, 74; Grt, 98; garnet peridotite xenolith: WR, 190 (major element), 41 (REE); Ol, 187; Cpx, 177 (major element), 61 (REE); Opx, 198; Grt, 231 (major element), 81(REE). Orogenic garnet peridotite: WR, 70 (major element), 26 (REE); Ol, 108; Cpx, 124 (major element), 24 (REE); Opx, 120; Grt, 226 (major element), 48 (REE). Composition of continental garnet peridotite xenolith estimated from average of modes and mineral compositions (Maaloe and Aoki 1977); Composition of spinel lherzolite xenolith refers to the average of 301 continental spinel lherzolites (Maaloe and Aoki 1977). Composition of primitive mantle is from Sun and McDonough (1989)

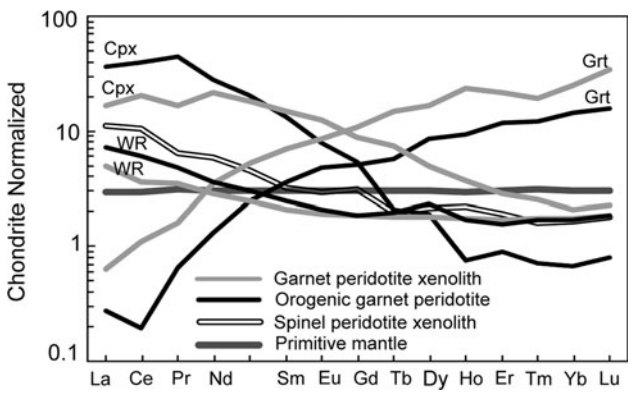

Fig. 10 Comparison of the average REE composition of primitive mantle, spinel peridotite xenolith and Cpx, Grt and whole rock of garnet peridotite. Chondrite-normalized values are the same as in Fig. 9

highly fractionated feature of cratonic garnet peridotite xenoliths. (4) Orogenic garnet peridotites are characterized by low T and large P variation, off-cratonic by high T and low P and cratonic by positive correlation between T and P. (5) Garnet peridotite xenoliths are of Archean or Proterozoic origin, whereas most of orogenic garnet peridotites are of Phanerozoic origin. As presented earlier, we suggest that at least three aspects, including tectonic setting, host rock and temporal evolution, are perhaps responsible for these features.

The lithosphere beneath cratons basically has a great thickness with low heat flow (e.g., Griffin et al. 1992; Kopylova and Caro 2004); thus, garnet peridotites could remain stable in a medium T and high P condition from Archean to Cenozoic, as suggested by P–T estimates particularly for those in kimberlite. Among off-craton areas, Kenya, Namibia and Buffalo, Canada are located in the margin of cratons and still have very thick lithosphere at present (Bishop et al. 1978; Henjes Kunst and Altherr 1992; Liati et al. 2004; Boyd et al. 2004; Kopylova and Caro 2004), so the garnet peridotite xenoliths from these areas plot in the craton field regardless of their host rocks. On the other hand, all the kimberlite fields but Namibia and Buffalo, Canada, outcrop in cratonic settings and all the other host rocks occur in off-craton settings except these localities in North China craton beneath which the lithosphere were subjected to large-scale thinning of up to 60–80 km at present (Griffin et al. 1992; Menzies et al. 1993; Xu et al. 1996, 2003; Fan et al. 2000; Zheng et al. 2004; Zhang 2005; Ying et al. 2006; Chen et al. 2006; Zhang et al. 2006, 2007a, b, 2008). It seems that the nature of

volcanic rocks highly depends on the thickness of lithosphere. However, further study is necessary to understand the correlations between the origin of volcanic rock and the lithospheric thickness. It is worth noting that ultra-mafic rock-hosting (low-Al) and mafic rock-hosting (high-Al) garnet peridotite xenoliths are mostly dominated by cratonic and off-cratonic xenoliths, respectively (Figs. 4c, 5a, b, 9).

A fact documented by abundant studies is that the lithospheric mantle had experienced multi-stage modification from Archean to Cenozoic evidenced by seismic mapping, wide-spreading volcanic rocks and xenoliths (e.g., Griffin et al. 1992; Beyer et al. 2006; Chen et al. 2006; Zheng et al. 2006; Zhang et al. 2006, 2007a, b, 2008; Su et al. 2009, 2010). All dated garnet peridotite xenoliths in Phanerozoic volcanic rocks record Archean or Proterozoic age, which makes it difficult to understand the temporal evolution. Absence of Phanerozoic garnet peridotite xenoliths possibly reveals no newly accreted garnet peridotite in Phanerozoic period or not being sampled so far. However, numerous Phanerozoic ages are preserved in orogenic garnet peridotites (Table 1). The efforts of plotting geochemical and mineral chemical items versus dated ages (not shown here) were specifically done, but we did not find any evolutional tendency. It is likely attributed to lack of precise analytical dating techniques and adequate datasets. In any case, the discovery of Phanerozoic garnet peridotite xenoliths has been a necessary step to understand the temporal evolution of the lithospheric mantle. On the other hand, alternative interpretation is that tectonic setting takes great responsibility for the compositional differences and it triggers us to argue specific questions about these Phanerozoic orogenic garnet peridotites: (1) were the records they preserved covered by the subsequent tectonic events? and (2) did they originate from the lithospheric mantle?

Exhumed mechanism of orogenic garnet peridotite

The garnet peridotites outcropping in orogenic belts which are assumed to have experienced subduction, collision and metamorphism, are basically suggested to record some information of deep lithosphere and even asthenosphere (Van Roermund et al. 2001; Zhang et al. 2003; Liou et al. 2004; Spengler et al. 2006; Medaris et al. 2005; Yang et al. 2007; Song et al. 2007). We are trying to find some geochronological, geochemical and thermal clues to the origin of orogenic garnet peridotites via comparisons to xenoliths.

Al_2O_3 and CaO contents in whole rock could mirror the degree of partial melting (Frey and Prinz 1978; Hellebrand et al. 2001). Relatively high and large Al_2O_3 ? CaO content range of orogenic garnet peridotite indicates low degree of melt extraction or modification due to the orogenic processes. Lithospheric material could possibly subduct into depth greater than 200 km (Van Roermund and Drury 1998, 2001; Ye et al. 2000). During the subduction process, increasing temperature plays a key role in structure and composition of the subducting lithosphere such as dehydration and melting (Kesson and Ringwood 1989). Experimental studies suggested that Al_2O_3 content in orthopyroxene decreases with the increasing temperature (Boyd 1973) and CaO, Cr_2O_3, Al_2O_3 and Cr# of pyroxene are sensitive indicators to pressure and temperature (Carroll Webb and Wood 1986; Brey and Kohler 1990). Orthopyroxenes in orogenic garnet peridotites with the same high-temperature feature as off-cratonic garnet peridotite xenoliths have the highest Al_2O_3 contents (Figs. 4c, 9), whereas CaO and Cr_2O_3 in orthopyroxenes and Al_2O_3 and CaO in clinopyroxenes also display the high contents (Figs. 4a, b, 5a–c). Besides, the orogenic garnet peridotites show increasing temperature with the decreasing CaO, Al_2O_3, TiO_2 and Cr_2O_3 contents of orthopyroxenes (Figs. 4, 9). These features reveal that these oxide contents are strongly affected by the temperature. The melt/fluid perhaps generated from dehydration of crustal material metasomatized the lithospheric mantle within the slab resulting in the formation of clinopyroxene with high LREE abundances and highly refractory.

After the slab was sequestered in asthenosphere perhaps for a very long period, some drive-mechanisms, unknown at present, brought them into the orogenic belt and mixed/came in contact with crustal materials. Due to the great strength of the collision, the orogenic belt produced high to ultra-high pressure. Previous studies suggested that Cr# of minerals of peridotites strongly depends on the pressure (Preb et al. 1986; Fan et al. 1997; Klemme and O'Neill 2000; Klemme 2004; Su et al. 2007). Cr# variations of pyroxenes shown in Figs. 4d, 5d are consistent with the pressure (Fig. 9), although Al_2O_3 and Cr_2O_3 contents decrease (Figs. 4b, c, 5b). The metamorphic condition of high to ultra-high pressure in orogenic belts is an ideal system to generate high-pressure minerals including coesite, diamond and garnet (Van Roermund et al. 2001; Zhang et al. 2003, 2004a, b; Yang 2003; Song et al. 2007). Garnets in crustal protoliths such as granulite and eclogite have low Mg# generally less than 70, whereas garnets in garnet peridotite xenoliths generally have the Mg# variation of 77–89 (Fig. 6a–c). Therefore, most of the garnets with medium Mg# in orogenic peridotites are likely to form from the mixture of crustal and mantle materials in the metamorphic process. Further support for these suggestions is that the orogenic garnets have an apparent Ce-negative anomaly which is assumed to result from interaction between crustal sediments and mantle peridotites (Luo et al. 2004) and Ce anomalies in Gough island lavas result from a recycled sediment component (Class and Roex

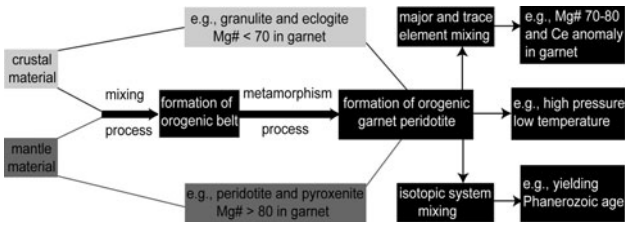

Fig. 11 Crust-mantle material mixing model for exhumed mechanism of orogenic garnet peridotite

2007). Many researchers attributed negative Yb anomaly of clinopyroxene to the crustal metasomatism (Rampone and Morten 2001; Zhang et al. 2003; Zheng et al. 2005). Isotopic systems might be also disturbed during the above-mentioned processes , otherwise, orogenic garnet peridotites should have given an older age than orogenic events. However, they usually have the same age (Table 1). This is an important clue to explain why many Phanerozoic garnet peridotites are merely found in orogenic belts rather than as xenoliths in volcanic rocks.

Based on the earlier discussion, a crust-mantle mixing model for the mechanism of orogenic garnet peridotite exhumation could be proposed and is shown in Fig. 11. Alps and Sulu-Dabie mountains are the typical and important orogenic garnet peridotite distributing areas (Fig. 1) and have been studied in more detail (e.g., Obata and Morten 1987; Green et al. 1997; Nimis and Morten 2000; Li 1994; Zhang et al. 1994; Xu et al. 2001, 2002; Yang et al. 2007). The TRANSALP Working Group (2002) proposed a crocodile model of the lithospheric structure beneath Eastern Alps. Meanwhile, the crocodile-like seismic profile of the lithospheric structure beneath Sulu-Dabie was reconstructed based on geophysical data by Li (1994), Lin (1995), Xu et al. (2001, 2002). Figure 12 compiles both relatively similar crocodile models, which provide an ideal tectonic setting for crustal and mantle material mixing process.

Geochronology of garnet peridotite

Generally, garnet peridotite xenoliths were subjected to a long-term evolution including partial melting, metasomatism and deformation etc. However, the whole rocks and their minerals such as clinopyroxene, garnet and minor zircon usually give the same or similar formation age even in different isotopic systems. The dated peridotite xenoliths always give relatively older ages, Archean and Proterozoic, compared to their host rocks, Cenozoic basalts or even Proterozoic kimberlites (Table 1). Consequently, many researchers do not date anymore xenoliths because the results cannot predict the evolution of the lithospheric mantle but rather concentrate attention on the host rocks from different periods. A typical example is the garnet peridotite xenoliths from Lashaine, Tanzania, which have been dated by U-Th-Pb, Rb-Sr, Sm-Nd and Re-Os isotopic systems (e.g., Hutchison and Dawson 1970; Cohen et al. 1984; Burton et al. 2000). The isotopic results of whole rocks and silicate minerals have the oldest Archean age, representing their formation period. On the other hand, the Re-Os results in sul des, which were interpreted to be metasomatic minerals, constrain the metasomatic age (Chesley et al. 1999; Burton et al. 2000), which reveals the evolution of the lithospheric mantle in another dimension. Since it is easy to nd hydrous and/or recrystallized minerals in mantle xenoliths, further detailed information about lithospheric mantle will be exploited in a future geochronological study. But rst of all, the issues why garnet peridotite xenoliths were formed nly in Archean or Proterozoic and why there is no newly accreted lithospheric mantle during Phanerozoic period in global scale should be considered.

As discussed previously, compared to garnet peridotite xenoliths, orogenic garnet peridotites experienced more complicated processes, especially high/ultrahigh-pressure metamorphism and mixing with crustal materials. Many studies suggested that the evolutional stages of some orogenic garnet peridotites could be described, e.g., from garnet phase to spinel phase and then back to garnet phase, or from spinel phase to garnet phase (e.g., Zhang and Liou 1998; Zhang et al. 2000a, b, 2003; Yang and Jahn 2000; Yang et al. 2007). Moreover, the similar dated ages of orogenic garnet peridotites with orogenic belts indicate that they could preserve very few records of origin of their protoliths. Although some differences in trace elements are

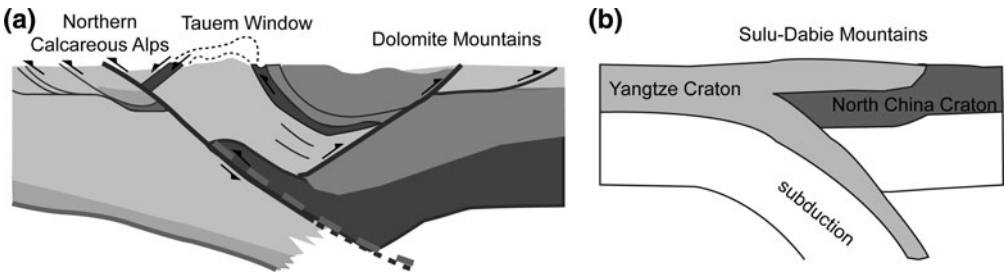

Fig. 12 Crocodile-like structure of lithosphere beneath Eastern Alps (after TRANSALP Working Group 2002) and Sulu-Dabie (modi ed after Lin 1995; Xu et al. 2001, 2002)

largely due to metasomatism, clinopyroxenes in orogenic garnet peridotites have relatively similar major element composition to those in garnet peridotite xenoliths (Fig. 5). Thus, clinopyroxenes could provide a basis to investigate the original formation of orogenic peridotites. Besides, high/ultrahigh-pressure minerals such as diamond inclusions in garnets and apatite probably give a clue to trace evolutional path of the orogenic garnet peridotites (e.g., Zhang et al. 2004a, b; Song et al. 2005, 2007).

Conclusion

1. Garnet peridotite xenoliths and orogenic garnet peridotites partly differ from each other in mineral and bulk compositions, and estimated pressure and temperature. In particular, Al_2O_3 content of pyroxenes in xenoliths is an important indicator to distinguish their origin and separate xenolith into low-Al and high-Al groups correlated with pressure and temperature. Garnet compositions are quite different between xenolith and orogenic garnet peridotite. Their outcropping tectonic setting should play a critical role in their differences.
2. Combining this study with previous estimation, the compositions involving major element and the REE of the global lithospheric mantle are compared with different estimations and further constrained. This estimation perhaps provides more precise data and a natural comparable standard composition to reveal the global and local evolution.
3. According to the compositional and age comparisons between garnet peridotite xenolith and orogenic garnet peridotite, a new model for exhumation of orogenic peridotite, crustal and mantle material mixing model is proposed and could be supported by the tectonic structure of the outcropping area (e.g., Eastern Alps and Sulu-Dabie).
4. Geochronological study on garnet peridotite should be an attractive and noticeable issue to understand the global spatial and temporal evolution of lithospheric mantle and to investigate metamorphic events and exhumed mechanisms of the orogenic garnet peridotite lenses/massifs.

Acknowledgments This research was nancially supported by the Knowledge Innovation Program of the Chinese Academy of Sciences (Grant KZCX2-YW-103), the National Science Foundation of China (Grants 90714008, and 40721062) and the grant from the University of Hong Kong. The authors would like to extend their sincere gratitude to the editors, Wolf-Christian Dullo and Wenjiao Xiao and two anonymous reviewers for editorial handling and constructive comments.

References

Abbott RN Jr, Draper G (2007) Petrogenesis of UHP eclogite from the Cuaba geneiss, Rio San Juan complex, Dominican Republic. Int Geol Rev 49:1069–1093

Abbott RN Jr, Broman BN, Draper G (2005a) UHP magma paragenesis revisited, olivine clinopyroxenite and garnet-bearing ultrama c rocks from the Cuaba gneiss, Rio San Juan complex, Dominican Republic. Int Geol Rev 49:572–586

Abbott RN Jr, Draper G, Keshav S (2005b) UHP magma paragenesis, garnet peridotite and garnet clinopyroxenite: an example from the Dominican Republic. Int Geol Rev 47:233–247

Abbott RN Jr, Draper G, Broman BN (2006) P–T path for ultra high pressure garnet ultrama c rocks of the Cuaba Gneiss, Rio San Juan Complex, Dominican Republic. Int Geol Rev 48:778–790

Altherr R, Kalt A (1996) Metamorphic evolution of ultrahigh-pressure garnet peridotites from the Variscan Vosges Mts. (France). Chem Geol 134:27–47

Aulbach S, Grif n WL, O'Reilly SY, McCandless TE (2004) Genesis and evolution of the lithospheric mantle beneath the Buffalo Head Terrane, Alberta (Canada). Lithos 77:413–451

Becker H (1996) Geochemistry of garnet peridotite massifs from lower Austria and the composition of deep lithosphere beneath a Palaeozoic convergent plate margin. Chem Geol 134:49–65

Beyer EE, Grif n WL, O'Reilly SY (2006) Transformation of Archaean lithospheric mantle by refertilization: evidence from exposed peridotites in the Western Gneiss Region, Norway. J Petrol 47:1611–1636

Bishop FC, Smith JV, Dawson JB (1978) Na, K, P and Ti in garnet, pyroxene and olivine from peridotite and eclogite xenoliths from African kimberlites. Lithos 11:155–173

Bizzarro M, Stevenson RK (2003) Major element composition of the lithospheric mantle under the North Atlantic craton: evidence from peridotite xenoliths of the Sarfartoq area, southwestern Greenland. Contrib Mineral Petrol 146:223–240

Boutelier D, Chemenda A, Jorand C (2004) Continental subduction and exhumation of high-pressure rocks: insights from thermo-mechanical laboratory modelling. Earth Planet Sci Lett 222:209–216

Boyd FR (1973) A pyroxene geotherm. Geochim Cosmochim Acta 37:2533–2546

Boyd FR, Pearson DG, Hoal KO, Hoal BG, Nixon PH, Kingston MJ, Mertzman SA (2004) Garnet lherzolite from Louwrensia, Namibia: bulk composition and P/T relations. Lithos 2004: 573–592

Brey GP, Kohler T (1990) Geothermobarometry in four-phase lherzolites II, new thermobarometers and pratical assessment of existing thermobarmeters. J Petrol 31:1353–1378

Brueckner HK, Roermund H, Pearson NJ (2004) An Archean (?) to Paleozoic evolution for a garnet peridotite lens with sub-baltic shield af nity within the Seve Nappe complex of Jamtland, Sweden, Central Scandinavian Caledonides. J Petrol 45:415–437

Burov E, Jolivet L, Le Pourhiet L, Poliakov A (2001) A thermomechanical model of exhumation of high pressure (HP) and ultra-high pressure (UHP) metamorphic rocks in Alpine-type collision belts. Tectonophysics 342:113–136

Burton KW, Schiano P, Birck JL, Allegre CJ, Rehkamper M, Halliday AN, Dawson JB (2000) The distribution and behavior of rhenium and osmium amongst mantle minerals and the age of the lithospheric mantle beneath Tanzania. Earth Planet Sci Lett 183:93–106

Cao RL, Zhu SH (1990) Ryacolite-olivine-diopside mineral assemblages of mantle metasomatism in garnet lherzolite xenolith from Xilong, Zhejiang province. Professional committee for mantle mineralogy, petrology and geochemistry under China

Society of Mineralogy, Petrology and Geochemistry. Collected papers on upper mantle characteristics and dynamics of China. Seismological Publishing House, Beijing, pp 34–44 (in Chinese with English abstract)

Carlson RW, Araujo AL, Junqueira-Brod TC, Gaspar JC, Brod JA, Petrinovic IA, Hollanda MHBM, Pimentel MM, Sichel S (2007) Chemical and isotopic relationship between peridotite xenoliths and ma c-ultrapotassic rocks from Southern Brazil. Chem Geol 242:418–437

Carroll Webb SA, Wood BJ (1986) Spinel-pyroxene-garnet relationship and their dependence on Cr/Al ratio. Contrib Mineral Petrol 77:185–194

Chemenda AI, Mattauer M, Bokum AN (1996) Continental subduction and a mechanism for exhumation of high-pressure metamorphic rocks: new modelling and eld data from Oman. Earth Planet Sci Lett 143:173–182

Chen L, Zheng TY, Xu WW (2006) A thinned lithospheric image of the Tanlu Fault Zone, eastern China: constructed from wave equation based receiver function migration. J Geophys Res 111:1–15

Chesley JT, Rudnick RL, Lee CT (1999) Re-Os systematics of mantle xenoliths from the East African Rift: age, structure, and history of the Tanzania craton. Geochim Cosmochim Acta 63:1203–1217

Chopin C (1984) Coesite and pure pyrope in high-grade blueschists of the western Alps: a rst record and some consequences. Contrib Mineral Petrol 86:107–118

Class C, Roex AP (2007) Ce anomalies in Gough island lavas—trace element characteristics of a recycled sediment component. Earth Planet Sci Lett doi10.1016/j.epsl.2007.10.030

Cohen RS, O'Nions RK, Dawson JB (1984) Isotope geochemistry of xenoliths from East Africa: implications for development of mantle reservoirs and their interaction. Earth Planet Sci Lett 68:209–220

Deng FL, Macdougall JD (1992) Proterozoic depletion of the lithosphere recorded in mantle xenoliths from Inner Mongolia. Nature 360:333–336

Downes H (1990) Shear zones in the upper mantle—relation between geochemical enrichment and deformation in mantle peridotites. Geology 18:374–377

Draper G, Nagle F (1991) Geology, structure and tectonic development of the Rio San Juan Complex, northern Dominican Republic. In: Mann P, Draper G, Lewis JF (eds) Geologic and tectonic development of the North American-Caribbean plate boundary in Hispaniola. Geological Society of America Special Paper, vol 262, pp 77–95

E ML, Zhao DS (1987) Cenozoic basalts and deep-seated xenoliths in eastern China. Science Press, Beijing (in Chinese)

Ehrenberg SN (1982) Petrogenesis of garnet lherzolite and mega crystalline nodules from the Thumb, Navajo volcanic eld. J Petrol 23:507–547

Enami M, Mizukami T, Yokoyama K (2004) Metamorphic evolution of garnet-bearing ultrama c rocks from the Gongen area, Sanbagawa belt, Japan. J Metamorph Geol 22:1–15

Fan QC, Hooper PR (1989) The mineral chemistry of ultrama c xenoliths of eastern China: implications for upper mantle composition and the paleogeotherms. J Petrol 30:1117–1158

Fan QC, Liu RX (1990) Study on phase transition of multiple spinel garnet peridotite in upper mantle beneath Eastern China. Professional committee for mantle mineralogy, petrology and geochemistry under China Society of Mineralogy, Petrology and Geochemistry. Collected papers on upper mantle characteristics and dynamics of China. Seismological Publishing House, Beijing, pp 72–82 (in Chinese)

Fan QC, Liu RX (1994) Spinel-garnet lherzolite in late tertiary limburgitic pipe from Hebi, Henan Province and its genesis. New progress in mineralogy, petrology and geochemistry study in China. Lanzhou University Press, pp 141–142 (in Chinese)

Fan QC, Liu RX, Xie HS, Zhang YM, Xu P, Lin ZR (1997) Experimental study of spinel-garnet phase transition in upper mantle and its signi cance. Sci China (D) 27:109–114

Fan WM, Zhang HF, Baker J, Mason PRD, Menzies MA (2000) On and off the North China craton: where is the Archean keel? J Petrol 41:933–950

Foley SF, Andronikov AV, Jacob DE, Melzer S (2006) Evidence from Antarctic mantle peridotite xenoliths for changes in mineralogy, geochemistry and geothermal gradients beneath a developing rift. Geochim Cosmochim Acta 70:3096–3120

Frey FA, Prinz M (1978) Ultrama c inclusions from San Carlos, Arizona: petrologic and geochemical data bearing on their petrogenesis. Earth Planet Sci Lett 38:129–176

Gao S, Rudnick RL, Carlson RW, McDonough WF, Liu YS (2002) Re-Os evidence for replacement of ancient mantle lithosphere beneath the North China craton. Earth Planet Sci Lett 198:307–322

Glaser SM, Foley SF, Gunther D (1999) Trace element compositions of minerals in garnet and spinel peridotite xenoliths from the Vitim volcanic eld, Transbaikalia, eastern Siberia. Lithos 48:263–285

Godard G, Martin S (2000) Petrogenesis of kelyphites in garnet peridotites: a case study from the Ulten zone, Italian Alps. J Geodyn 30:117–145

Godard G, Martin S, Prosser G, Kieneast JR, Morten L (1996) Variscan migmatites, eclogites and garnet-peridotites of the Ulten zone, eastern Austroalpine system. Tectonophysics 259:313–341

Green HW, Dobrzhinetskaya L, Riggs EM, Jin ZM (1997) Alpe Arami: a peridotite massif from the mantle transition zone? Tectonophysics 279:1–21

Grif n WL, O'Reilly SY, Ryan CG (1992) Composition and thermal structure of the lithosphere beneath South Africa, Siberia and China: proton microprobe studies, international symposium on Cenozoic volcanic rocks and deep-seated xenoliths of China and its environs, Beijing, 20

Grif n WL, Natapov LM, O'Reilly SY, Achterbergh EV, Cherenkova AF, Cherenkov VG (2005) The Kharamai kimberlite eld, Siberia: modi cation of the lithospheric mantle by the Siberian trap event. Lithos 81:167–187

Hacker BR, Sharp T, Zhang RY, Liou JG, Hervig RL (1997) Determining the origin of ultrahigh-pressure lherzolites. Science 278:702–704

Hellebrand E, Snow JE, Dick HJB, Hofmann AW (2001) Coupled major and trace elements as indicators of the extent of melting in mid-ocean-ridge peridotites. Nature 410:677–681

Helmers H, Maaskant P, Hartel THD (1990) Garnet peridotite and associated high-grade rocks from Sulawesi, Indonesia. Lithos 25:171–188

Henjes Kunst F, Altherr R (1992) Metamorphic petrology of xenoliths from Kenya and Northern Tanzania and implications for geotherms and lithospheric structures. J Petrol 33:1125–1156

Hood CTS, McCandless TE (2004) Systematic variations in xenocryst mineral composition at the province scale, Buffalo Hills kimberlites, Alberta, Canada. Lithos 77:733–747

Huang XL, Xu XS, Cai YF, Zhou XM (1998) Deep-seated xenoliths in Nushan alkali-basalts, Anhui Province. J Nanjing Univ (Nat Sci) 34:292–302 (in Chinese with English abstract)

Hunter WC, Smith D (1981) Garnet peridotite from Colorado Plateau ultrama c diatremes: hydrates, carbonates and comparative geothermometry. Contrib Mineral Petrol 76:312–320

Hutchison R, Dawson JB (1970) Rb, Sr and $^{87}Sr/^{86}Sr$ in ultrabasic xenoliths and host-rocks, Lashaine volcano, Tanzania. Earth Planet Sci Lett 9:87–92

Ionov DA (2004) Chemical variations in peridotite xenoliths from Vitim, Siberia: inferences for REE and Hf behavior in the garnet-facies upper mantle. J Petrol 45:343–367

Ionov DA, Ashchepkov IV, Stosch HG, Witt-Eickschen G, Seck HA (1993) Garnet peridotite xenoliths from the Vitim volcanic field, Baikal region: the nature of the garnet-spinel peridotite transition zone in the continental mantle. J Petrol 34:1141–1175

Ionov DA, Ashchepkov IV, Jagoutz E (2005) The provenance of fertile off-craton lithospheric mantle: Sr-Nd isotope and chemical composition of garnet and spinel peridotite xenoliths from Vitim, Siberia. Chem Geol 217:41–75

Isozaki Y, Maruyama S, Furuoka F (1990) Accreted oceanic materials in Japan. Tectonophysics 181:179–206

Jahn BM (1998) Geochemical and isotopic characteristics of UHP eclogites of the Dabie orogen: implications for continental subduction and collisional tectonics. In: Hacker B, Liou JG (eds) When continents collide: geodynamics and geochemistry of ultrahigh-pressure rocks, pp 203–239

Jahn BM, Wu FY, Lo CH, Tsai CH (1999) Crust-mantle interaction induced by deep subduction of the continental crust: geochemical and Sr-Nd isotopic evidence from post-collisional mafic-ultramafic intrusions of the northern Dabie complex, central China. Chem Geol 157:119–146

Janak M, Froitzheim N, Vrabec M, Ravna EJK, Hoog JCMD (2006) Ultrahigh-pressure metamorphism and exhumation of garnet peridotite in Pohorje, eastern Alps. J Metamorph Geol 24:19–31

Jin SY, Pan SA (1998) Mantle-derived xenoliths of spinel-garnet lherzolite from Nushan and their implications for petro-physics. Earth Sci J China Univ Geosci 23:475–479 (in Chinese with English abstract)

Junqueira Brod TC, Gaspar JC, Brod JA, Kafino CV (2005) Kamafugitic diatremes: their textures and field relationships with examples from the Goia's alkaline province, Brazil. J S Am Earth Sci 18:337–353

Kadarusman A, Parkinson CD (2000) Petrology and P–T evolution of garnet peridotites from central Sulawesi, Indonesia. J Metamorph Geol 18:193–209

Kawato K, Isozaki Y, Itaya T (1991) Geotectonic boundary between the Sanbagawa and Chichibu belts in central Southwest Japan. J Geol Soc Jpn 97:959–975 (in Japanese with English abstract)

Kerrich R, Polat A (2006) Archean greenstone-tonalite duality: thermochemical mantle convection models or plate tectonics in the early Earth global dynamics? Tectonophysics 415:141–165

Kesson SE, Ringwood AE (1989) Slab-mantle interactions 1, sheared and refertilised garnet peridotite xenoliths—samples of Wadati-Benioff zones? Chem Geol 78:83–96

Klemme S (2004) The influence of Cr on the garnet-spinel transition in the Earth's mantle: experiments in the system MgO–Cr_2O_3–SiO_2 and thermodynamic modeling. Lithos 77:639–646

Klemme S, O'Neill HSC (2000) The effect of Cr on the solubility of Al in orthopyroxene: experiments and thermodynamic modelling. Contrib Mineral Petrol 140:84–98

Kopylova MG, Caro G (2004) Mantle xenoliths from the southeastern Slave craton: evidence for chemical zonation in a thick, cold lithosphere. J Petrol 45:1045–1067

Kopylova MG, O'Reilly SY, Genshaft YS (1995) Thermal state of the lithosphere beneath Central Mongolia: evidence from deep-seated xenoliths from the Shavaryn-Saram volcanic centre in the Tariat depression, Hangai, Mongolia. Lithos 36:243–255

Lenoir X, Garrido CJ, Bodinier JL, Dautria JM, Gervilla F (2001) The recrystallization front of the Ronda peridotite: evidence for melting and thermal erosion of subcontinental lithospheric mantle beneath the Alboran Basin. J Petrol 42:141–158

Li ZX (1994) Collision between the North and South China blocks: a crustal-detachment model for suturing in the region east of the Tanlu fault. Geology 22:739–742

Li TF, Ma HW, Bai ZM (1999) Temperature and pressure states of spinel-garnet transition zone beneath Hannuoba area. Geoscience 13:66–72 (in Chinese with English abstract)

Liati A, Franz L, Gebauer D, Fanning CM (2004) The timing of mantle and crustal events in South Namibia, as defined by SHRIMP-dating of zircon domains from a garnet peridotite xenoliths of the Gibeon kimberlite province. J Afr Earth Sc 39:147–157

Lin SF (1995) Collision between the North and South China blocks: a crustal-detachment model for suturing in the region east of the Tanlu fault: comment. Geology 23:574–575

Lin CY, Shi LB, Chen XD, Zhang XO, Xu YG, Mercier JC (1995) Rheological features of garnet lherzolite xenoliths from Xinchang, Zhejiang province, China and their geological implications. Acta Petrol Sin 11:55–64 (in Chinese with English abstract)

Liou JG, Zhang RY (1998) Petrogenesis of ultrahigh-P garnet-bearing ultramafic body from Maowu, the Dabie Mountains, Central China. Isl Arc 7:115–134

Liou JG, Tsujimori T, Zhang RY, Katayama I, Maruyama S (2004) Global UHP metamorphism and continental subduction/collision: the Himalayan model. Int Geol Rev 46:1–27

Liou JG, Zhang RY, Ernst WG (2007) High-pressure geosciences special feature: very high-pressure orogenic garnet peridotites. High Press Geosci 104:9116–9121

Litasov KD, Foley SF, Litasov YD (2000) Magmatic modification and metasomatism of the subcontinental mantle beneath the Vitim volcanic field (East Siberia): evidence from trace element data on pyroxenite and peridotite xenoliths from Miocene picrobasalt. Lithos 54:83–114

Liu RX, Fan QC, Sun JZ (1985) Study on garnet lherzolite xenoliths from eastern China. Acta Petrol Sin 1:24–33 (in Chinese)

Liu RX, Fan QC, Li HM, Zhang Q, Zhao DS, Ma BL (1995) The nature of protolith of Bixiling garnet peridotite-eclogite massif in Dabie mountains and the implication of its isotopic geochronology. Acta Petrol Sin 11:243–256 (in Chinese with English abstract)

Luo Y, Gao S, Yuan HL, Liu XM, Deltlef G, Jin ZM, Sun M (2004) Ce anomaly in minerals of eclogite and garnet pyroxenite from Dabie-Sulu ultrahigh pressure metamorphic belt: tracking subducted sediment formed under oxidizing conditions. Sci China (D) 34:920–930

Maaloe S, Aoki K (1977) The major element composition of the upper mantle estimated from the composition of lherzolites. Contrib Mineral Petrol 63:161–173

MacKenzie JM, Canil D, Johnston S, English J, Mihalynuk MG, Grant B (2005) First evidence for ultrahigh-pressure garnet peridotite in the North American Cordillera. Geol Soc Am 33:105–108

McDonough WF (1990) Constraints on the composition of the continental lithospheric mantle. Earth Planet Sci Lett 101:1–18

McDonough WF, Frey FA (1989) REE in upper mantle rocks. In: Lipin B, McKay GR (eds) Geochemistry and mineralogy of rare earth elements. Mineral Society of American, pp 99–145

McDonough WF, Stosch HS, Ware NG (1992) Distribution of titanium and the rare earth elements between peridotitic minerals. Contrib Mineral Petrol 110:321–328

Medaris G, Wang H, Jelinek E, Mihaljevic M, Jakes P (2005) Characteristics and origin of diverse Variscan peridotites in the Gfohl Nappe, Bohemian Massif, Czech Republic. Lithos 82:1–23

Menzies MA, Chazot G (1995) Fluid processes in diamond to spinel facies shallow mantle. J Geodyn 20:387–415

Menzies MA, Hawkesworth CJ (1987) Mantle metasomatism. Academic Press, London, p 472

Menzies MA, Fan WM, Zhang M (1993) Paleozoic and Cenozoic lithoprobes and the loss of 120 km of Archean lithosphere, Sino-Korean craton, China. In: Prichard HM, Alabaster T, Harris NBW, Neary CR (eds) Magmatic processes and plate tectonics. Geological Society Special Publication, vol 76, pp 71–81

Menzies A, Westerlund K, Grutter H, Gurney J, Carlson J, Fung A, Nowicki T (2004) Peridotitic mantle xenoliths from kimberlites on the Ekati Diamond Mine property, N.W.T., Canada: major element compositions and implications for the lithosphere beneath the central Slave craton. Lithos 77:395–412

Morishita T, Arai S, Gervilla F (2001) High-pressure aluminous ma c rocks from the Ronda peridotite massif, southern Spain: signi cance of sapphirine- and corundum-bearing mineral assemblages. Lithos 57:143–161

Nimis P, Morten L (2000) P–T evolution of 'crustal' garnet peridotites and included pyroxenites from Nonsberg area (upper Austroalpine), NE Italy: from the wedge to the slab. Geodynamics 30:93–115

Nimis P, Trommsdorff V (2001) Revised thermobarometry of Alpe Arami and other garnet peridotites from the central Alps. J Petrol 42:103–115

Obata M (1980) The Ronda peridotite: garnet-, spinel-, and plagioclase-lherzolite facies and the P–T trajectories of a high-temperature mantle intrusion. J Petrol 21:533–572

Obata M, Morten L (1987) Transformation of spinel lherzolite to garnet lherzolite in ultrama c lenses of the Austridic Crystalline Complex, Northern Italy. J Petrol 28:599–623

Ota T, Gladkochub DP, Sklyarov EV, Mazukabzov AM, Watanabe T (2004) P–T history of garnet-websterites in the Sharyzhalgai complex, southwestern margin of Siberian Craton: evidence for Paleoproterozoic high-pressure metamorphism. Precambr Res 132:327–348

Paquin J, Altherr R (2001) New constraints on the P–T evolution of the Alpe Arami garnet peridotite body (central Alps, Switzerland). J Petrol 42:1119–1140

Preb S, Witt G, Seck HA, Eonov D, Kovalenko (1986) Spinel peridotite xenoliths from the Tariat depression, Mongolia: major element chemistry and mineralogy of a primitive mantle xenolith suite. Geochim Cosmochim Acta 50:2587–2599

Rampone E, Morten L (2001) Records of crustal metasomatism in the garnet peridotites of the Ulten zone (upper Austroalpine, eastern Alps). J Petrol 42:207–219

Reid AM, Donaldson CH, Brown RW, Ridley WI, Dawson JB (1975) Mineral chemistry of peridotite xenoliths from the Lashaine volcano, Tanzania. Phys Chem Earth 9:525–543

Rhodes JM, Dawson JB (1975) Major and trace element chemistry of peridotite inclusions from the Lashaine volcano, Tanzania. Phys Chem Earth 9:545–557

Ridley WI, Dawson JB (1975) Lithophile trace element data bearing on the origin of peridotite xenoliths, ankaramite and carbonatite from the Lashaine volcano, Tanzania. Phys Chem Earth 9:559–569

Roden MF, Shimizu N (2000) Trace element abundances in mantle-derived minerals which bear on compositional complexities in the lithosphere of the Colorado Plateau. Chem Geol 165:283–305

Sagong H, Kwon ST, Cheong CS, Choi SH (2001) Geochemical and isotopic studies of the Cretaceous igneous rocks in the Yeongdong Basin, Korea: implications for the origin of magmatism in pull-apart basin. Geochem J 5:191–201

Salters VJM (1996) The generation of mid-ocean ridge basalts from the Hf and Nd isotope perspective. Earth Planet Sci Lett 141:109–123

Saltzer RL, Chatterjee N, Grove TL (2001) The spatial distribution of garnets and pyroxenes in mantle peridotites: pressure-temperature history of peridotites from the Kaapvaal Craton. J Petrol 42:2215–2229

Schiano P, Eiler JM, Hutcheon ID, Stolper EM (2000) Primitive CaO-rich, silica-undersaturated melts in island arcs: evidence for the involvement of clinopyroxene-rich lithologies in the petrogenesis of arc magmas. Geochemistry, Geophysics, Geosystems, 1999GC000032

Schmidberger SS, Francis D (1999) Nature of the mantle roots beneath the North American craton: mantle xenolith evidence from Somerset Island kimberlites. Lithos 48:195–216

Simon NSC, Irvine GJ, Davies GR, Pearson DG, Carlson RW (2003) The origin of garnet and clinopyroxene in "depleted" Kaapvaal peridotites. Lithos 71:289–322

Smith DC (1984) Coesite in clinopyroxene in the Caledonides and its implications for geodynamics. Nature 310:641–644

Smith D, Ehrenberg SN (1984) Zoned minerals in garnet peridotite nodules from the Colorado Plateau: implications for mantle metasomatism and kinetics. Contrib Mineral Petrol 86:274–285

Smith D, Grif n WL, Ryan CG, Sie SH (1991) Trace element zonation in garnets from The Thumb: heating and melt in ltration beneath the Colorado Plateau. Contrib Mineral Petrol 107:60–79

Song SG, Zhang LF, Niu YL (2004) Ultra-deep origin of garnet peridotite from the North Qaidam ultrahigh-pressure belt, Northern Tibetan Plateau, NW China. Am Mineral 89:1330–1336

Song SG, Zhang LF, Niu YL, Su L, Jian P, Liu DY (2005) Geochronology of diamond-bearing zircons from garnet peridotite in the North Qaidam UHPM belt, Northern Tibetan Plateau: a record of complex histories from oceanic lithosphere subduction to continental collision. Earth Planet Sci Lett 234:99–118

Song SG, Su L, Niu YL, Zhang LF, Zhang GB (2007) Petrological and geochemical constraints on the origin of garnet peridotite in the North Qaidam ultrahigh-pressure metamorphic belt, northwestern China. Lithos 96:243–265

Spengler D, Roermund HLM, Drury MR, Ottolini L, Mason PRD, Davies GR (2006) Deep origin and hot melting of an Archaean orogenic peridotite massif in Norway. Nature 440:913–917

Stern CR, Kilian R, Olker B, Hauri EH, Kyser TK (1999) Evidence from mantle xenoliths for relatively thin (100 km) continental lithosphere below the Phanerozoic crust of southernmost South America. Lithos 48:217–235

Stosch HG (1982) Rare earth element partitioning between minerals from anhydrous spinel peridotite xenolith. Geochim Cosmochim Acta 46:793–811

Su BX, Zhang HF, Xiao Y, Zhao XM (2006) Characteristics and geological signi cance of olivine xenocrysts in Cenozoic volcanic rocks from western Qinling. Prog Nat Sci 16:1300–1306

Su BX, Zhang HF, Wang QY, Sun H, Xiao Y, Ying JF (2007) Spinel-garnet phase transition zone of Cenozoic lithospheric mantle beneath the eastern China and western Qinling and its T-P condition. Acta Petrol Sin 23:1313–1320 (in Chinese with English abstract)

Su BX, Zhang HF, Ying JF, Xiao Y, Zhao XM (2009) Nature and mantle processes of the lithospheric mantle beneath the western Qinling: evidence from deformed peridotitic xenoliths entrained in Cenozoic kamafugite from Haoti, Gansu Province, China. J Asian Earth Sci 34:258–274

Su BX, Zhang HF, Sakyi PA, Ying JF, Tang YJ, Yang YH, Qin KZ, Xiao Y, Zhao XM (2010) Compositionally strati ed lithosphere and carbonatite metasomatism recorded in mantle xenoliths from the Western Qinling (Central China). Lithos doi:10.1016/j.lithos.2010.01.004

Sun SS, McDonough WF (1989) Chemical and isotopic systematic of oceanic basalts: implications for mantle composition and processes. In: Saunders AD, Norry MJ (eds) Magmatism in the Ocean basins. Geological Society Special Publication, vol 42, pp 313–345

Tang YJ, Zhang HF, Ying JF (2006) Asthenosphere-lithospheric mantle interaction in an extensional regime: Implication from the geochemistry of Cenozoic basalts from Taihang Mountains, North China Craton. Chem Geol 233:309–327

TRANSALP Working Group (2002) First deep seismic re ection images of the Eastern Alps reveal giant crustal wedges and transcrustal ramps. Geophys Res Lett 29 doi:10.1029/2002GL014911

Van Roermund HLM, Drury MR (1998) Ultra-high pressure (P > 6 GPa) garnet peridotites in western Norway: exhumation of mantle rocks from more than 185 km. Terra Nova 10:295–301

Van Roermund HLM, Drury MR, Barnhoorn A, Ronde AD (2001) Relict majoritic garnet microstructures from ultra-deep orogenic peridotites in Western Norway. J Petrol 42:117–130

Viljoen KS, Schulze DJ, Quadling AG (2005) Contrasting group I and Group II eclogite xenolith petrogenesis: petrological, trace element and isotopic evidence from eclogite, garnet-websterite and alkremite xenoliths in the Kaalvallei kimberlite, South Africa. J Petrol 46:2059–2090

Villasante-Marcos V, Osete ML, Gervilla F, Garcia-Duenas V (2003) Palaeomagnetic study of the Ronda peridotites (Betic Cordillera, southern Spain). Tectonophysics 377:119–141

Warren CJ, Beaumont C, Jamieson RA (2008) Modelling tectonic styles and ultra-high pressure (UHP) rock exhumation during the transition from oceanic subduction to continental collision. Earth Planet Sci Lett 267:129–145

Wu FY, Walker RJ, Yang YH, Yuan HL, Yang JH (2006) The chemical-temporal evolution of lithospheric mantle underlying the North China craton. Geochim Cosmochim Acta 70:5013–5034

Xu YG (2000) Distribution of trace elements in spinel and garnet peridotites. Sci China (D) 30:307–314

Xu XS, O'Reilly SY, Zhou XM, Grif n WL (1996) A xenoliths-derived geotherm and the crust-mantle boundary at Qilin, southeastern China. Lithos 38:41–62

Xu XS, O'Reilly SY, Grif n WL, Zhou XM, Huang XL (1998) The nature of the Cenozoic lithosphere at Nushan, Eastern China. In: Mantle dynamics and plate interactions in East Asia, Geodynamics, vol 27, American Geological Union, pp 167–195

Xu PF, Liu FT, Wang QC, Cong BL, Chen H (2001) Slab-like high velocity anomaly in the uppermost mantle beneath the Dabie-Sulu orogen. Geophys Res Lett 28:1847–1850

Xu PF, Liu FT, Ye K, Wang QC, Cong BL, Chen H (2002) Flake tectonics in the Sulu orogen in eastern China as revealed by seismic tomography. Geophys Res Lett 29 doi:10.1029/2001GL014185

Xu XS, O'Reilly SY, Grif n WL, Zhou XM (2003) Enrichment of upper mantle peridotite: petrological, trace element and isotopic evidence in xenoliths from SE China. Chem Geol 198:163–188

Xu ZQ, Wang Q, Ji SC, Chen J, Zeng LS, Yang JS, Chen FY, Liang FH, Wenk HR (2006) Petrofabrics and seismic properties of garnet peridotite from the UHP Sulu terrane (China): implications for olivine deformation mechanism in a cold and dry subducting continental slab. Tectonophysics 421:111–127

Yamamoto H, Okamoto K, Kaneko Y, Terabayashi M (2004) Southward extrusion of eclogite-bearing ma c-ultrama c bodies in the Sanbagawa belt, central Shikoku, Japan. Tectonophysics 387:151–168

Yang JJ (2003) Titanian clinohumite-garnet-pyroxene rock from the Sulu UHP metamorphic terrane, China: chemical evolution and tectonic implications. Lithos 70:359–379

Yang JS, Jahn BM (2000) Deep subduction of mantle-derived garnet peridotites from the Sulu UHP metamorphic terrane in China. J Metamorph Geol 18:167–180

Yang JS, Zhang RY, Li TF, Zhang ZM, Liou JG (2007) Petrogenesis of the garnet peridotite and garnet-free peridotite of the Zhimafang ultrama c body in the Sulu ultrahigh-pressure metamorphic belt, eastern China. J Metamorph Geol 25:187–206

Ye K, Cong BL, Ye DN (2000) The possible subduction of continental material to depth greater than 200 km. Nature 407:734–736

Ying JF, Zhang HF, Kita N, Morishita Y, Shimoda G (2006) Nature and evolution of Late Cretaceous lithospheric mantle beneath the eastern North China craton: constraints from petrology and geochemistry of peridotitic xenoliths from Jiaodong, Shandong Province, China. Earth Planet Sci Lett 244:622–638

Yoshida D, Hirajima T, Ishiwatari A (2004) Pressure-temperature path recorded in the Yangkou garnet peridotite, in Sulu Ultrahigh-pressure metamorphic belt, eastern China. J Petrol 45:1125–1145

You ZD, Zhong ZQ, Suo ST, Zheng S (2000) A petrogenetic study of the garnet pyroxenite enclaves in spinel peridotite, North Dabieshan, China. Sci China (D) 30:108–115

Yu XH (2004) Kamafugites: a younger hot topic in the igneous petrology. Geoscience 18:449–453 (in Chinese with English abstract)

Yu XH, Mo XX, Liao ZL, Zhao X, Su Q (2001) Temperature and pressure condition of garnet lherzolite and websterite from west Qinling, China. Sci China (D) 44:155–161

Zhang HF (2005) Transformation of lithospheric mantle through peridotite-melt reaction: a case of Sino-Korean craton. Earth Planet Sci Lett 237:768–780

Zhang RY, Cong BL (1985) The geotherm and constituent of uppermost mantle derived from xenoliths in southeastern China. Acta Petrol Sin 1:34–49 (in Chinese)

Zhang RY, Liou JG (1998) Dual origin of garnet peridotites of the Dabie-Sulu UHP terrane, eastern-central China. Episodes 21:229–234

Zhang RY, Liou JG, Cong BL (1994) Petrogenesis of garnet-bearing ultrama c rocks and associated eclogites in the Sulu ultrahigh-P metamorphic terrane, eastern China. J Metamorph Geol 12:169–186

Zhang HF, Menzies MA, Lu FX, Zhou XH (2000a) Major and trace element studies on garnet from Palaeozoic kimberlite-borne mantle xenoliths and megacrysts from the North China craton. Sci China (D) 43:423–430

Zhang RY, Liou JG, Yang JS, Yui TF (2000b) Petrochemical constraints for dual origin of garnet peridotites from the Dabie-Sulu UHP terrane, eastern-central China. J Metamorph Geol 18:149–166

Zhang HF, Sun M, Lu FX, Zhou XH, Zhou MF, Liu YS, Zhang GH (2001) Geochemical signi cance of a garnet lherzolite from the Dahongshan kimberlite, Yangtze Craton, southern China. Geochem J 35:315–331

Zhang RY, Liou JG, Yang JS, Ye K (2003) Ultrahigh-pressure metamorphism in the forbidden zone: the Xugou garnet peridotite, Sulu terrane, eastern China. J Metamorph Geol 21:539–550

Zhang RY, Liou JG, Yang JS, Li L, Jahn BM (2004a) Garnet peridotites in UHP mountain belts of China. Int Geol Rev 46:981–1004

Zhang RY, Liou JG, Zheng JP (2004b) Ultrahigh-pressure corundum-rich garnetite in garnet peridotite, Sulu terrane, China. Contrib Mineral Petrol 147:21–31

Zhang RY, Yang JS, Wooden JL, Liou JG, Li TF (2005) U-Pb SHRIMP geochronology of zircon in garnet peridotite from the Sulu UHP terrane, China: implications for mantle metasomatism and subduction-zone UHP metamorphism. Earth Planet Sci Lett 237:729–743

Zhang HF, Ying JF, Tang YJ, Zhang J, Zhao XM, Niu LF, Xiao Y, Su BX (2006) Heterogeneity of Mesozoic and Cenozoic lithospheric mantle beneath the eastern North China Craton: evidence from

olivine compositional mapping. Acta Petrol Sin 22:2279–2288 (in Chinese with English abstract)

Zhang HF, Nakamura E, Kobayashi K, Zhang J, Ying JF, Tang YJ, Niu LF (2007a) Transformation of subcontinental lithospheric mantle through deformation-enhanced peridotite-melt reaction: evidence from a highly fertile mantle xenolith from the North China craton. Int Geol Rev 49:658–679

Zhang HF, Ying JF, Shimoda G, Kita NT, Morishita Y, Shao JA, Tang YJ (2007b) Importance of melt circulation and crust-mantle interaction in the lithospheric evolution beneath the North China Craton: evidence from Mesozoic basalt-borne clinopyroxene xenocrysts and pyroxenite xenoliths. Lithos 96:67–89

Zhang RY, Li T, Rumble D, Yui TF, Li L, Yang JS, Pan Y, Liou JG (2007c) Multiple metasomatism in Sulu ultrahigh-P garnet peridotite constrained by petrological and geochemical investigations. J Metamorph Geol 25:149–164

Zhang HF, Goldstein SL, Zhou XH, Sun M, Zheng JP, Cai Y (2008) Evolution of subcontinental lithospheric mantle beneath eastern China: Re-Os isotopic evidence from mantle xenoliths in Paleozoic kimberlites and Mesozoic basalts. Contrib Mineral Petrol 155:271–293

Zhao RX, Liou JG, Tsujimori T, Zhang RY (2007) Petrology and U-Pb SHRIMP geochronology of a garnet peridotite, Sulu UHP terrane, east-central China. Int Geol Rev 49:732–752

Zheng JP, O'Reilly SY, Grif n WL, Zhang M, Lu FX, Liu GL (2004) Nature and evolution of Mesozoic-Cenozoic lithospheric mantle beneath the Cathaysia block, SE China. Lithos 74:41–65

Zheng JP, Zhang RY, Grif n WL, Liou JG, O'Reilly SY (2005) Heterogeneous and metasomatized mantle recorded by trace elements in minerals of the Donghai garnet peridotites, Sulu UHP terrane, China. Chem Geol 221:243–259

Zheng JP, Grif n WL, O'Reilly SY, Yang JS, Li TF, Zhang M, Zhang RY, Liou JG (2006) Mineral chemistry of peridotites from Paleozoic, Mesozoic and Cenozoic lithosphere: constraints on mantle evolution beneath eastern China. J Petrol 47:2233–2256

Zhi XC (2000) Re-Os isotopic system and formation age of subcontinental lithospheric mantle. Chin Sci Bull 45:193–200

Zhi XC, Qin X (2004) Re-Os isotope geochemistry of the mantle-derived peridotite xenoliths from eastern China: constrains on the age and thinning of lithospheric mantle. Acta Petrol Sin 20:989–998 (in Chinese with English abstract)

Zhi XC, Peng ZC, Chen DG, Yu CJ, Sun WD, Reisberg L (2001) The longevity of subcontinental lithospheric mantle beneath Jiangsu-Anhui region. Sci China (D) 44:1110–1118